Review

Construction and Application of DNAzyme-based Nanodevices

WANG Bo[1#], WANG Menghui[1#], PENG Fangqi[1#], FU Xiaoyi[3], WEN Mei[1], SHI Yuyan[1], CHEN Mei[2], KE Guoliang[1✉] and ZHANG Xiao-Bing[1✉]

Received December 9, 2022
Accepted January 2, 2023

The development of stimuli-responsive nanodevices with high efficiency and specificity is very important in biosensing, drug delivery, and so on. DNAzymes are a class of DNA molecules with the specific catalytic activity. Owing to their unique catalytic activity and easy design and synthesis, the construction and application of DNAzymes-based nanodevices have attracted much attention in recent years. In this review, the classification and properties of DNAzyme are first introduced. The construction of several common kinds of DNAzyme-based nanodevices, such as DNA motors, signal amplifiers, and logic gates, is then systematically summarized. We also introduce the application of DNAzyme-based nanodevices in sensing and therapeutic fields. In addition, current limitations and future directions are discussed.

Keywords DNAzyme; Nanodevice; Biosensor; Therapy

1 Introduction

In the past few decades, many kinds of molecule nanodevices with mechanical and electronic characteristics on the microscale have been developed. These various nanodevices can sense given external signals and perform specific, highly complex functions. Such stimuli-responsive nanodevices have great potential for various applications in biosensing, programmable drug delivery, and biocomputing.

As we all know, DNA carries genetic information. Beyond that, DNA is one of the most promising biomolecules in material science and nanotechnology for future applications. The specificity of the A-T and G-C Watson-Crick base-pairing interactions provides a method to construct diverse DNA formations of programmed structures and sequences. Rational design and fabrication of synthetic nanodevices, which can realize biological operations has become one of the most fascinating research topics of nanotechnology. Recently, various artificial DNA-based nanodevices have been reported in response to certain inputs, which holds great prospect for performing diverse biological applications, such as biosensing[1−3], therapy[4−6], cellular network mimicking[7,8], and biocomputing[9,10].

DNAzymes are a sort of catalytic nucleic acids created through *in vitro* selection processes, by which specific substrates could be cleaved in the presence of cofactors[11−13]. Breaker and Joyce[14] discovered the first kind of DNAzyme in the presence of Pb^{2+} which was able to catalyze a transesterification reaction in 1994 through a process that was called *in vitro* selection. The result demonstrated that single strand DNA could indeed act as a catalyst, which is similar to proteins and ribozymes. Since then, a series of DNAzymes that are specific for biomacromolecules[15], metal ions[14,16−18], and small molecules[19,20] has been selected. One of the advantages of DNAzymes is amenability to specific applications, as they can be engineered artistically to fit different needs. Secondly, DNAzyme shows excellent specificity for its substrate strand. Even one single base mismatch in the catalytic core will decrease the cleaving activity significantly. In addition, DNAzymes are highly programmable, since the binding arms are modified and functionalized easily. This makes these DNAzymes not only outstanding signal amplifiers for biosensing or versatile recognition elements but also promising mRNA-targeted therapeutics. In addition to the RNA-cleaving DNAzymes mentioned above, there is another kind of DNAzyme named hemin/G-quadruplex-DNAzyme, which could employ hemin to imitate the peroxidase activity and oxidize 2,2-azino-bis-(3-ethylben-zthiazoline-6-sulfonic acid)(ABTS) to generate color change or selectively catalyze luminol/H_2O_2 to produce chemiluminescence(CL).

DNAzymes are emerging as a highly programmable component for the design of molecular nanodevices, which can perform complex tasks including sensing[1,2,21], controlled drug release[22−24], target gene silencing[25−29], and biological computing[9]. In the review, we briefly introduce the classification and features of DNAzymes. Then, the construction of several kinds of DNAzyme-based nanodevices including walkers, tweezers, signal amplifiers, logic gates, and constitutional dynamic networks(CDN) is summarized. Subsequently, the discussion focuses on the emerging biological application of DNAzyme-based nanodevices in biosensing and therapy. Finally, current challenges and opportunities of DNAzyme-based nanodevices are discussed.

✉ KE Guoliang
glke@hnu.edu.cn
✉ ZHANG Xiao-Bing
xbzhang@hnu.edu.cn
# These authors contributed equally to this work.
1. State Key Laboratory of Chemo/Biosensing and Chemometrics, College of Chemistry and Chemical Engineering, Hunan University, Changsha 410082, P. R. China;
2. College of Materials Science and Engineering, Hunan University, Changsha 410082, P. R. China;
3. Institute of Basic Medicine and Cancer(IBMC), Chinese Academy of Sciences, Hangzhou 310022, P. R. China

https://doi.org/10.1007/s40242-023-2334-8

2 Types of DNAzymes

2.1 RNA-cleaving DNAzymes

In the past research, a series of DNAzymes had been selected to catalyze numerous biological reactions, such as oligonucleotide cleavage[16,30], ligation[31−33], and phosphorylation reactions[34−36]. Substrate types of DNAzymes used for cleaving include DNA and RNA. Lu's group[37] reported peptide nucleic acid(PNA)-assisted double-stranded DNA nicking by DNAzymes(PANDA), which extended the substrate of DNAzyme to dsDNA. RNA-cleaving DNAzymes represent the best catalytic activity and may even be the most widely used DNAzymes available at present, which can be divided into two categories: DNAzymes, which can cleave full-RNA substrates and cleave RNA-DNA chimeras. The classification between cleavage substrates is particularly important for different applications. For example, the RNA-DNA chimera cleaving DNAzyme may not be practical for therapeutic applications, but it is the optimal option in sensing applications[38].

The mechanism of RNA cleavage by DNAzymes is similar to ribozymes[39]. As shown in Fig.1(A), the 2′ hydroxyl becomes deprotonated as the catalytic cation stabilizes developed charge on the 3′ and 5′ oxygens, then a phosphodiester linkage transfers to a 2′,3′ cyclic phosphate and a 5′ hydroxyl is produced after protonation[40]. Among all DNAzymes, the 10-23 and 8-17 DNAzymes are the two most widely used DNAzymes with full RNA as catalytic substrates[16]. The 10-23 DNAzyme denoted as R-Y in Fig.1(B) can cleave sites containing purine-pyrimidine junctions, and yet the 8-17 DNAzyme restrictively cleaves between N-G junction[17]. In the presence of 50 mmol/L Mg^{2+}, this DNAzyme shows much higher(10^5-fold of K_m) RNA-cleaving activity than protein enzyme ribonuclease A. The K_m and catalytic efficiency of this DNAzymes are calculated to be 0.76 nmol/L and 3.2×10^9 $mol\cdot L^{-1}\cdot min^{-1}$, respectively[17,18]. The 10-23 DNAzyme has the fastest catalytic cleavage rates(10^9 $mol\cdot L^{-1}\cdot min^{-1}$) of RNA-cleaving DNAzyme, which gives it the possibility of application in the field of biosensing[13,41]. In addition, several other common DNAzymes have been reported, which shows dependence on different metal ions. For example, Joyce and co-workers[42] reported a Mg^{2+}- and Na^+-specific DNAzyme named E6. Subsequently, Lu's group[43] reported a Pb^{2+}-dependent DNAzyme named 17E. The rate constant(K_{obs}) with 100 μmol/L Pb^{2+} was determined to be 5.75 min^{-1} at pH 6.0. After that, a Na^+-dependent DNAzyme named NaA43(K_{obs} *ca*. 0.1 min^{-1}), containing 8-17's conserved bases, was reported by Lu's group[44] and considered to be only bound to Na^+ until Ce^{3+}-dependent catalytic activity was found by Liu's group[45].

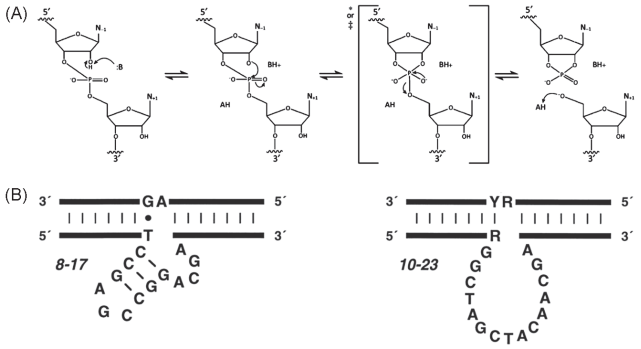

Fig.1 Schematic illustration of transesterification reaction catalyzed by RNA-cleaving DNAzymes(A) and secondary structure of 8-17 DNAzyme(left) and 10-23 DNAzyme(right)(B)
(A) Reprinted with permission from Ref.[40], Copyright 1998, American Chemical Society; (B) reprinted with permission from Ref.[17], Copyright 1997, American Chemical Society.

So, they also named the DNAzyme with the same catalytic core sequence as Ce13d. In their research, it has been proven that the catalytic activity of NaA43 is dependent on Na^+ and could be promoted by Ce^{3+}. Correspondingly, Ce^{3+}-dependent cleavage activity of Ce13d could be accelerated by Na^+[45].

Since the sequence of the two binding arms in DNAzyme will not affect the catalytic activity, the reasonable designing binding arms with different sequences can identify different target nucleic acid sequences of interest. This flexible and highly programmable characteristic gives RNA-cleaving DNAzymes versatility in biosensing applications.

2.2 Hemin/G-Quadruplex DNAzyme

Another kind of DNAzyme is hemin/G-quadruplex DNAzyme. The G-quadruplex was first reported by Gellert *et al*. in 1962[46]. The G-rich sequence will fold into parallel or anti-parallel G-quadruplex under allosteric activation by K^+, Pb^{2+}, or NH^{4+} through intermolecular or intramolecular hoogsteen hydrogen bonds. As shown in Fig.2(A), the G-quadruplex is composed of one, two, or four DNA molecules, which have many different topologies, depending on the number and orientation of the G-rich DNA strands[47]. The first DNAzymes with peroxidase-mimicking activity were reported by Sen's group[48,49]. As shown in Fig.2(B), G-quadruplex can bind to hemin to form hemin/G-quadruplex complexes featured with peroxidase-mimicking activity[49,50]. Its tentative mechanism is shown in Fig.2(C), and axial ligands of iron in hemin can allosterically bind to the G-quadruplex, followed by transient interactions between iron in hemin and oxygen in guanine, facilitating electron transfer reaction in this catalytic system[51]. Cheng's group[52] explored the connection between peroxidase-mimicking activity and different topological G-quadruplex structures. The intramolecular parallel G-quadruplex showed

https://doi.org/10.1007/s40242-023-2334-8

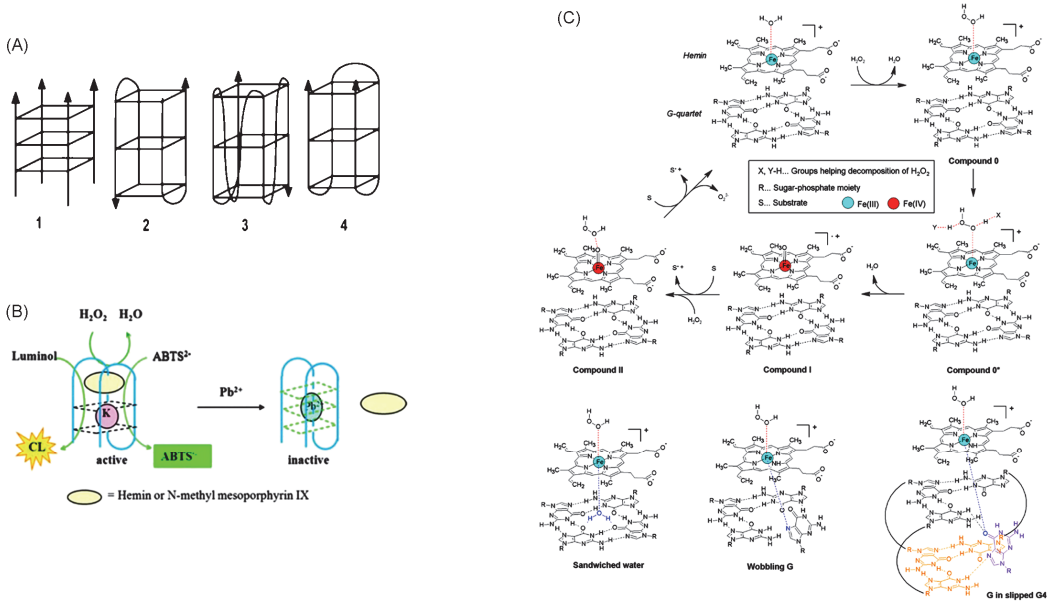

Fig.2 Scheme of four kinds G-quadruplex structures: (1) parallel tetramolecular, (2) antiparallel bimolecular, (3) parallel unimolecular, (4) antiparallel unimolecular(A), G-quadruplex binding to hemin to form hemin/G-quadruplex DNAzyme with peroxidase-mimicking activity(B), and catalytic mechanism of the hemin/G-quadruplex DNAzyme(C)

(A) Reprinted with permission from Ref.[47], Copyright 2011, Elsevier; (B) reprinted with permission from Ref.[50], Copyright 2015, The Royal Society of Chemistry; (C) reprinted with permission from Ref.[51], Copyright 2021, American Chemical Society.

high enzymatic activity because this topological structure was conducive to the end stacking of hemin. Furthermore, Shen's group[53,54] also proved that the intramolecular parallel structure showed much more peroxidase-mimicking activity than the antiparallel structure, even the interaction of hemin could promote the variation of some G-quadruplexes from antiparallel to parallel conformation.

To improve the enzymatic activity of hemin/G-quadruplex DNAzyme, a series of strategies has been developed[55—61]. For example, Xiang's group[62] synthesized cationic peptide conjugates of hemin/G-quadruplex DNAzymes, which showed peroxidase activities up to 4-fold than original DNAzymes.

With horseradish peroxidase(HRP)-mimicking activity, hemin/G-quadruplex DNAzymes could selectively catalyze H_2O_2 and oxidize luminol to generate chemiluminescence (CL)[63], or oxidize 2,2-azino-bis-(3-ethylben-zthiazoline-6-sulfonic acid)(ABTS) to produce a colorimetric signal[49]. Therefore, a series of hemin/G-quadruplex DNAzymes-based biosensors have been emerging in recent years[64—71].

3 Construction of DNAzyme-based Nanodevices

DNAzymes as an important class of functional DNA not only hold excellent recognition ability towards cofactors that can be used to construct biosensors but also have great potential for the design of gene silencing therapeutic nanodevices. By flexibly designing different arm sequences, DNAzymes can be used to design various kinds of nanodevices. According to its operating status, these DNAzyme-based nanodevices are classified into walkers, tweezers, signal amplifiers, logic gates, and constitutional dynamic networks(CDN).

3.1 DNAzyme-based Walker

DNA walkers as a distinct kind of dynamic DNA devices, where the nucleic acids or nanoparticles can walk along a programed-designed track, are inspired by naturally occurring molecular walkers, such as dynein, kinesin, and myosin. Due to its catalytic cleavage activity similar to that of nucleases, DNAzyme can be used to drive the movement of DNA walker. Driving the walking strand to move stably and procedurally along the track strands is the key to achieving the normal operation of DNA walkers. Depending on how the DNA walker moves, the categories of the tracks can be sorted into one-dimensional(1D) tracks, two-dimensional(2D) tracks, and three-dimensional(3D) tracks roughly.

3.1.1 1D Tracks

DNA double helix has been considered as a track for helping DNA walker directional moving with strand displacement reaction since Pierce[72] reported the pioneering work in 2004. Since then, many approaches have been reported to develop such DNA walkers. However, such DNA walkers need manual

operation and only move when the composition of the solution is changed or a DNA strand is added. To solve this problem, Mao's group[73] have designed a self-actuated autonomous DNA walker that could continuously walk without human operation or other external active elements. The walking mechanism of the novel walkers combines DNAzyme cleavage activity with a strand-displacement strategy. As shown in Fig.3(A), the walker is driven by a 10-23 DNAzyme, which consists of a catalytic core and two asymmetrical recognition arms. They chose DNA-RNA chimeras as the substrate chains. When the substrate chain is cut by DNAzyme, the free short arm will hybridize with the adjacent chimer as substrate track, thus driving the whole walker movement. The whole process can be repeated such that the DNAzyme moves constantly without human intervention.

Due to the thermodynamic instability of DNA double helix in the solution, in order to enhance the stability, they further constructed a 10-23 DNAzyme-based walker along single-walled carbon nanotubes to transport nanoparticles, such as CdS nanocrystals[74]. The RNA substrate strands were decorated on the single-walled carbon nanotubes. The DNAzyme continuously cleaves RNA substrate strand to drive autonomous, processive walking along the one-dimensional track, which consists of single-walled carbon nanotubes and RNA molecules. Carbon nanotubes have a longer distance to provide enough walking space and do not need to control the starting position compared with the DNA double helix short track[75]. Furthermore, the inherent near-infrared emission of the carbon-nanotube track also offers an effective way to visualize the movement of the individual walker in real time.

In addition, hemin/G-quadruplex DNAzymes can also be used for designing DNA walkers. Willner and coworkers[76] reported a DNA walker assembled on a DNA double helix track and triggered by an additional fuel/anti-fuel strand. The fuel or anti-fuel strand results in the reversible dissociation or the formation of the hemin/G-quadruplex DNAzyme on the track. With different designs, different signals can be generated, such as photoelectrochemical, transduction electrochemical, chemiluminescence, or chemiluminescence resonance energy transfer(CRET).

3.1.2 2D Tracks

Since the direction of motion of the DNA walkers traveling on 1D linear tracks has obvious limitations, the researchers, therefore, designed 2D planar tracks. Compared with 1D linear tracks, 2D planar tracks show one prominent advantage that they have higher dimensionality with adequate space for the immobilization of substrate molecules.

The construction of 2D tracks mainly relies on two-dimensional nanomaterials, such as gold electrodes(GE) and alkynylated glass slides[77]. The GE is easy to prepare and is regarded as a commonly used 2D track, on which *via* Au-S bonds the thiolated DNA can be modified. For example, Cao's group[78] proposed an electrochemical biosensing platform based on the target-triggered DNAzyme-based tripod walker for the detection of telomerase. This enzyme-free and polymerase chain reaction(PCR)-free electrochemical strategy showed a detection limit of 10 cells. Subsequently, in order to enhance the recognition efficiency, Miao *et al*.[79] further modified a number of tetrahedral DNA(TDNA) as supported tracks and walkers on the surface of GE.

In addition, the researchers also focused on the combination of aptamers and DNA walkers to further improve the specificity of the molecular recognition process. As a functional element, the aptamer can combine with multiple targets and have significant advantages in specificity and selectivity. Therefore, the design of molecular recognition unit based on aptamer can effectively improve the specificity of detection. One strategy is to activate blocked aptamer with DNAzymes. For example, Jie's team[80] has reported a versatile electrochemiluminescence(ECL) and a photoelectrochemical (PEC) biosensing strategy for the ultrasensitive detection of glutathione(GSH) by a Mn^{2+}-depended DNAzyme and DNA walker based allosteric conversion amplification of aptamer. As shown in Fig.3(B), GSH reduces the MnO_2 nanosheets to Mn^{2+}, and then the Mn^{2+} acts to produce a great number of short single strands(putput DNA) as a cofactor of DNAzyme. The output DNA triggered the track hairpin DNA, which was fixed on the Au electrode switched to an aptamer structure. Thus, the quantum dots(QDs, CdS:Mn), which were modified with streptavidin(SA) on the electrode by specific binding of SA to its aptamer generated PEC and ECL signals. Another design strategy is to use an aptamer to hybridize with the walker strand so that the walker can be blocked. Only when the target appears, can the walker be released to achieve the subsequent movement. For example, Wang's group[81] has designed a man-carried aptasensor, which was based on a DNA walker for the on-site detection in food matrixes of Aflatoxin B1(AFB1) with the readout of the personal glucose meter(PGM). A similar strategy is being used to detect MCF-7 cells with the limit of detection as low as 47 cells/mL[82].

3.1.3 3D Tracks

Although compared with the 1D track, the 2D track has been greatly improved in the space available for walk and substrate molecular modification, there is still a large room for improvement. Currently, with the continuous development of DNA nanotechnology and the increasing demand for further improvement of DNA walker performance, the 3D tracks came out as a matter of course. The 3D tracks having a strong

https://doi.org/10.1007/s40242-023-2334-8

capability of DNA loading are constructed on the micro- or nanoparticles' surface. The local probe's concentration on the surface is strikingly enhanced for better signal amplification efficiency and higher walking efficiency due to the large specific surface area of micro- or nanoparticles. At present, magnetic beads(MBs) and gold nanoparticles(AuNPs) have already been used to construct the DNAzyme-based 3D track. The MBs-based 3D track has been used for protein detection and metal ions detection[83]. For example, Zhou's group[84] has reported an ultrasensitive and universal fluorescence biosensor based on catalytic hairpin assembly(CHA) strategy and a 3D-bipedal DNA walker for thrombin detection with the limit of detection(LOD) as low as 23 fmol/L.

Besides, similar to the 2D gold electrodes, the 3D track based on AuNPs can be established on the surface of AuNPs by using the strong Au—S bond to modify the thiolated oligonucleotides, which can successfully achieve the stepwise and random movement of the DNA walker at the nanoscale space. Because of its excellent signal amplification characteristics, it can be used to detect *in vitro* targets, like thrombin[85], antigen[86], and Zika virus RNA[87]. However, it is still a challenge on AuNP surfaces to control the orientation and conformation of the 3D track accurately and adjust the 3D track hybridization ability finely. To solve this problem, He's group[88] designed a polyadenine(polyA)-based, spatially isolated 3D DNA track, where a target-activated DNAzyme walker moved with improved processivity and efficiency through a burnt-bridge mechanism.

Besides, the AuNPs also can act as the carriers to make 3D track operating in cells. For example, Le's group[89] designed a DNAzyme walk machine on an AuNP for real-time imaging of microRNA in living cells. As shown in Fig.3(C), the entire walking machine is built on 20-nm AuNPs which are decorated with dozens of silenced DNAzyme strandhybridized with locking strands and hundreds of substrate strands serving as DNA tracks. The target microRNA(miRNA) can hybridize with the blocking strand to activate Mn^{2+}-dependent DNAzyme. And then, the exogenous Mn^{2+} would initiate the autonomous walking of the machine on the AuNP surface. The entire system is highly integrated on a gold particle, which improves the cell uptake efficiency of the entire system. Furthermore, the structure of high-density tracks on AuNP leads to high walking speed that can accomplish 30 walking steps in 30 min. A similar exogenous Mn^{2+}-powered strategy was used to design the unipedal[90] and bipedal[91] DNA walker to detect intracellular miRNA.

To avoid adding exogenous metal cofactors, Zhang's group[92] proposed a Na^+-fueled DNAzyme walker inside the cell, which can differentiate non-small cell lung cancer (NSCLC) cell subtypes through profiling the miRNA biomarker. As shown in Fig.3(D), the Na^+-specific DNAzymes were locked, leading to low fluorescence signals without target miRNA. In the existence of target miRNA(miRNA-21 and miRNA-205), the DNAzymes would be active and cleave their substrates respectively. This Na^+-fueled DNAzyme walker inside the cell could distinguish cell subtypes of NSCLC through identifying the miRNA.

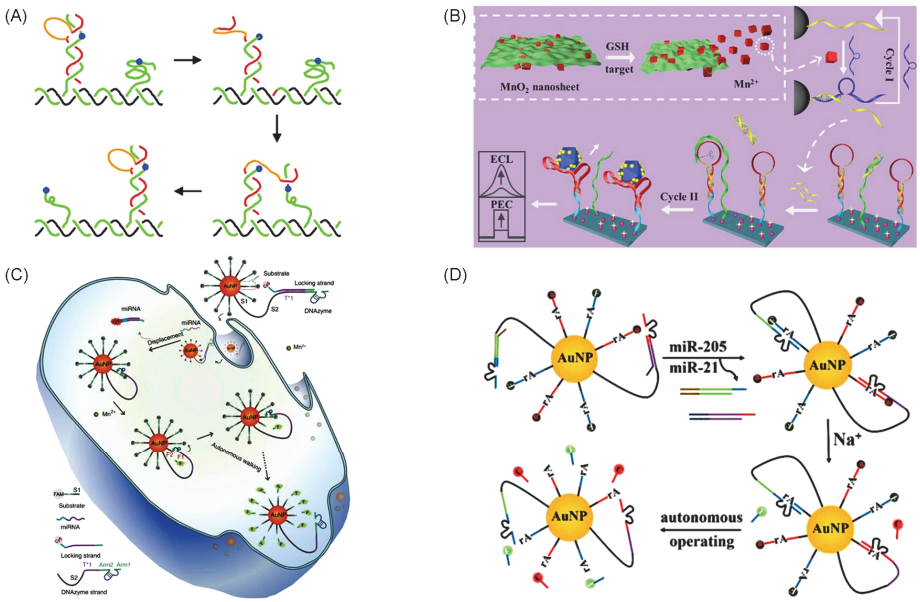

Fig.3 Schematic illustration of DNAzyme-based DNA walkers

(A) 1D tracks: self-actuated autonomous DNA walker without human operation or other external active elements. Reprinted with permission from Ref.[73], Copyright 2005, Wiley; (B) 2D tracks: activate blocked aptamer with DNAzymes. Reprinted with permission from Ref.[80], Copyright 2019, American Chemical Society; (C) 3D tracks: AuNPs used as carriers to make 3D tracks operating in cells. Reprinted with permission from Ref.[89], Copyright 2017, Springer Nature; (D) an intracellular Na^+-fueled DNAzyme walker to differentiate cell subtypes of NSCLC by profiling the miRNA biomarker. Reprinted with permission from Ref.[92], Copyright 2020, American Chemical Society.

https://doi.org/10.1007/s40242-023-2334-8

The exogenous driving force and weak biostability limit the operation of DNA walkers *in vivo*. In order to realize the body operation of the 3D track, Kong's group[93] further combined the Mn^{2+}-dependent DNAzyme-powered DNA motor with the MnO_2 nanosheet, which was triggered by GSH. Due to the outstanding biocompatibility of 3D DNA walker nanoprobe, Gao's group[94] proposed a DNAzyme-powered three-dimensional DNA walker nanoprobe for imaging Amyloid β-peptide oligomer(AβO) *in vivo*. Nie's group[95] developed a strategy, which could couple the nanoscale operation of a self-propelled DNA walker-type robot operating on the cell membrane(3D track) with precisely programmable cell functions, such as regulating cytoskeleton remodeling and MET/AKT signaling to enhance cell migration.

3.2 DNAzyme-based Tweezers

Similar to DNA walkers, inspired by the cellular protein motors, researchers have also developed a series of DNAzyme-based tweezer nanomotors. Mao's group[96] proposed an autonomous DNAzyme-based tweezer nanomotor, which integrated the 10-23 DNAzyme into a self-assembled DNA nanostructure. As shown in Fig.4(A), the integrated system is composed of two 15-base-pair double helix structures and the single DNAzyme strand of 10-23 DNAzyme. When there was no substrate strand binding to the DNAzyme, the DNAzyme strand would fold into a tight configuration("closed state"). In the presence of substrate strands, the hybridization of the substrate strands to DNAzyme led to the opening of the tweezer("open state"). After binding to the substrate strand, the substrate strand would be cleaved into two short fragments by the 10-23 DNAzyme and release the cleavage products, thus causing the tweezer into a "closed state" and binding to substrate strands again in the next cycle. The entire integrated system would automatically switch between the two states until the substrate strands in the solution ran out. Based on this integrated design strategy, Mao's group[97] further put a brake on the autonomous DNAzyme-based tweezer nanomotor to realize a reversible switch.

Based on the catalytic activity triggered by the presence of coenzyme factors, the DNAzyme-based nanotweezers have been used in the detection of biomolecules[98] and metal ions[99] widely. In addition, due to the cleavage characteristics of the substrate chain, it can also identify and act on nucleic acid targets. For example, Chu's group[100] proposed a multifunctional nanotweezer for sensing intracellular TK1 mRNA and gene silencing therapy. As shown in Fig.4(B), the end of the DNAzyme-based nanotweezer arm consists of the complementary sequence of split-DNAzyme segment and TK1 mRNA. The recognition of TK1 mRNA realized intracellular imaging of TK1 mRNA. At the same time, the hybridization led to the formation of complete DNAzyme structures to cleave survivin mRNA. TK1 mRNA activated the split-DNAzyme and achieved high specificity gene silencing therapy without side effects. RNA-cleaving DNAzyme-based nanotweezers would have enormous potential for the diagnosis and therapy of cancer with the characters of low immunogenicity,

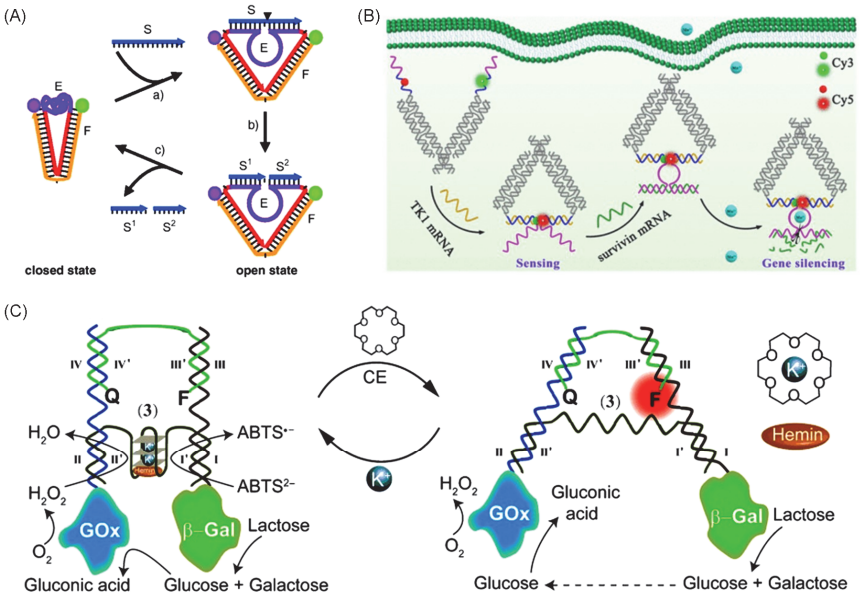

Fig.4 Schematic illustration of DNAzyme-based DNA tweezers

RNA cleaving DNAzyme-based tweezers: (A) an autonomous DNAzyme-based tweezer nanomotor. Reprinted with permission from Ref.[96], Copyright 2004, Wiley; (B) a multifunctional nanotweezer for sensing intracellular TK1 mRNA and gene silencing therapy. Reprinted with permission from Ref.[100], Copyright 2021, American Chemical Society; hemin/G-quadruplex DNAzyme-based tweezer: (C) an "ON/OFF" switchable tweezer structure controling enzymatic cascade. Reprinted with permission from Ref.[101], Copyright 2014, Wiley.

https://doi.org/10.1007/s40242-023-2334-8

remarkable biocompatibility, excellent specificity, and high programmability.

In another fantastic study, hemin/G-quadruplex DNAzyme was used to construct an "ON/OFF" switchable tweezer structure as a linker by Willner's group[101]. As shown in Fig.4(C), the formation of the hemin/G-quadruplex structure led to the closed configuration of the tweezers and biocatalytic cascades("ON"). In the existence of 18-crown-6-ether, the tweezers would be opened and the enzymatic cascade was inhibited("OFF").

3.3 DNAzyme-based Amplifier

Apart from being versatile elements of the above DNA motors, DNAzymes are also an outstanding component of signal amplifiers due to their "one-to-more" cleavage activity on the substrate chain or the construction of the hemin/G-quadruplex structure. Herein, DNAzymes are considered as highly suitable signal amplifiers and transducers for biosensing.

3.3.1 RNA-cleaving DNAzyme as the Signal Amplifier

DNAzymes show great application potential in detecting low-abundance targets based on signal amplification technology due to their specific target cleavage ability. By rational and ingenious design, DNAzymes can be used in the recognition of diverse kinds of targets besides their cofactors. In these signal transduction and amplification strategies, targets will activate DNAzymes and subsequently trigger the cleavage of substrates to realize signal amplification. For example, Ding's group[102] designed a homogeneous fluorescent biosensor for the detection of DNA. By ingenious combination of entropy-driven strand displacement reaction(ESDR) and Mg^{2+}-dependent DNAzyme, this sensor is enzyme-free and separation-free, and is made sensitive to detect target DNA in 90 min with a low LOD as 220 fmol/L. Similar to the above report, the target process-induced signal amplification strategy is used to build an ultrasensitive fluorescence biosensor for intracellular Pb^{2+} detection[103]. As shown in Fig.5(A), cofactor Pb^{2+} was used as the target, which could trigger the cleavage of the substrate with remarkable specificity and then released the DNAzyme and Pb^{2+}. The released Pb^{2+} would participate in the recycle again to achieve signal amplification. Meanwhile, the released DNAzyme would open the hairpin to trigger the intermediate recycling and a fluorescence signal could be generated. Under the best-case condition, the LOD was calculated to be 0.3 nmol/L.

However, it is difficult to meet the requirements of ultrasensitive detection with only DNAzyme-based methods, especially for intracellular target detection. Currently, in order to further enhance the sensitivity of target recognition, many efficient strategies that combine DNAzymes with other amplification methods have gained significant attention. In particular, rolling circle amplification(RCA), hybridization chain reaction(HCR), and catalytic hairpin assembly(CHA) are three widely used strategies for signal amplification, and all these strategies show excellent sensitivity. CHA is an enzyme-free signal amplification circuit. Based on this feature, CHA could achieve amplification simply through cascade DNA hybridization and strand displacement, making them applicable for nucleic acid amplification inside living cells. Lu's group[104] designed a CHA reaction based on photocaged Na^+-specific DNAzyme to detect intracellular Na^+ sensitively. As shown in Fig.5(B), upon simultaneous activation of exogenous light and endogenous Na^+, the DNAzyme would cleave the rA position in its substrate strand, and then the released initiator DNA(I) triggered the CHA amplification. Once the initiator DNA(I) was released, it would open the H1 through toehold-mediated hybridization. And then the second toehold sequence on H1 would sequentially open H2, and outputted a turn-on fluorescence signal. It was the first work of a DNAzyme sensor for detecting endogenous metal ions inside living cells.

In addition, HCR has been pervasively used in biosensors' development as an enzyme-free signal amplification method with excellent sensitivity and specificity[105]. For example, Huang's group[106] designed double-amplified cascaded logic DNA biocircuits for the identification of cancer cell subtypes with miR-122 and miR-21 as biomarkers. This strategy greatly improved sensitivity by cascading DNAzyme and improved veracity by simultaneous detection of dual cancer marker. Moreover, Wang's group[107] constructed an autocatalytic DNAzyme(ACD) circuit based on DNAzyme and HCR, for amplified microRNA imaging based on DNAzyme biocatalysis and HCR *in vivo*, sustained by a honeycomb MnO_2 nanosponge(hMNS). As shown in Fig.5(C), the hMNS can not only be used as the carrier of ACD biocircuit but also can degrade in the presence of GSH to produce Mn^{2+} as a cofactor of a magnetic resonance imaging(MRI) reagent and DNAzyme. After releasing DNA probes, the endogenous miRNA-21 triggers the HCR-mediated autonomous assembly of DNAzyme nanowires, by which the Mn^{2+}-mediated substrate cleavage could be catalyzed to generate new triggers for the initial HCR amplifier. The accurate localization of miRNA is realized by the robust hMNS/ACD system *in vivo*. An isothermal concatenated nucleic acid amplification system was also designed, which is composed of intermediate HCR, a lead-in CHA, and ultimate DNAzyme amplifier units[108]. This CHA-HCR-DNAzyme assay could realize intracellular imaging of miRNA in living cells, resulted from their synergetic signal amplifications. Wang's group[109] further

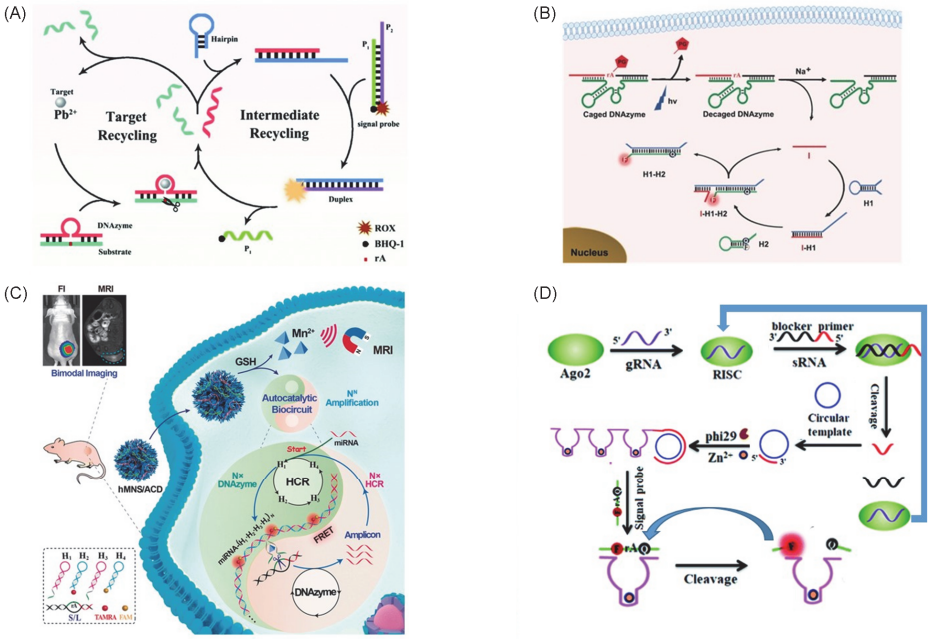

Fig.5 Schematic illustration of DNAzyme-based cleavage-induced signal amplification combined with other amplification methods

(A) ESDR. Reprinted with permission from Ref.[103], Copyright 2017, The Royal Society of Chemistry; (B) CHA. Reprinted with permission from Ref.[104]. Copyright 2017, Wiley; (C) HCR. Reprinted with permission from Ref.[107], Copyright 2020, Wiley; (D) RCA. Reprinted with permission from Ref.[110], Copyright 2018, The Royal Society of Chemistry.

designed a similar feedback HCR-DNAzyme system for amplified intracellular miRNA imaging.

RCA is also an isothermal nucleic acid amplification method, which often combined in the development of DNAzyme detection technology. Zhang's group[110] designed a DNAzyme biosensor based on the integration of RCA with an 8-17 DNAzyme for the detecting Argonaute 2(Ago2) with a LOD of 0.35 pmol/L. As shown in Fig.5(D), the cleavage of the substrate RNA could be initiated by the target Ago2 to produce a free RCA primer, and then the RCA reaction was triggered to synthesize a great deal of 8-17 DNAzymes, and the products, 8-17 DNAzymes, can cleave ample substrate probes to generate an amplified fluorescence signal. Benefiting from the dual-signal amplification design, the endogenous Ago2 activity can even be accurately measured in HeLa cell extracts with a detection limit as low as 3 cells.

3.3.2 Hemin/G-quadruplex DNAzyme as the Signal Amplifier

It has been reported that hemin could be combined to construct the hemin/G-quadruplex DNAzyme, which could mimic HRP through the G-quadruplex DNAzyme. Especially, compared to free hemin, hemin/G-quadruplex DNAzyme could produce 250-fold enhanced peroxidase activity. Thus, hemin/G-quadruplex DNAzyme was enabled to become an outstanding amplifier by the super catalytic properties for biosensor designing.

Hemin/G-quadruplex DNAzyme colorimetric biosensors have been reported in recent years due to their remarkable advantages, such as label-free, easy-preparation, and fast-reaction. The construction of hemin/G-quadruplex DNAzyme complex could trigger peroxidation with ABTS and H_2O_2, which could realize naked-eye detection. Kim's group[111] reported a specific and sensitive colorimetric assay used to analyze human norovirus genogroups I and II(HuNoV GI and GII) in the samples of oyster. The researchers used a toehold-mediated strand displacement reaction to further improve the signal amplification performance of the hemin/G-quadruplex DNAzyme colorimetric biosensors. Jia's group[112] reported an intelligent DNA machine based on cyclic nucleic acid strand displacement polymerization(CNDP) and the hemin/G-quadruplex DNAzyme mediated the signal readout with a detection limit as low as 10 fmol/L. A similar toehold-mediated strand displacement reaction was used to construct a colorimetric microRNA detection strategy[113].

Researchers have put forward many nucleic acids signal amplification techniques combined with hemin/G-quadruplex DNAzyme to promote the continuous development of the sensitivity of detection methods. For example, Xiao's group[114] proposed a multi-amplification nanoplatform for the visual detection of HIV DNA biomarkers in real physiological media with a detection limit as low as 4.8 pmol/L, which was based on the nanofibrous membrane and combined CHA

https://doi.org/10.1007/s40242-023-2334-8

amplification with hemin/G-quadruplex DNAzyme signal output. As shown in Fig.6(A), the target(HIV DNA) would trigger the CHA amplification, which could generate the H1-H2 double helices on the nanofibrous membrane surface. In the existence of H_2O_2, the oxidation of colorless $ABTS^{2-}$ could be catalyzed by the HRP-mimicking DNAzyme to produce a green color of $ABTS^{-}$. Yang's group[71] constructed a sensitive and versatile quantum dot(QD)-based "signal-off" electrochemiluminescence(ECL) sensing system with CHA amplification strategies and target-initiated dual Mg^{2+}-dependent DNAzyme recycling. The ECL of QDs could be quenched effectively by the hemin/G-quadruplex-Y-shaped DNA complexes. The constructed platform demonstrated outstanding sensitivity and detection limits as low as 0.28 pmol/L, 3.71 fmol/L, and 35.00 amol/L(S/N=3) for ion(Ag^{+} as a model), aptamer substrates(ATP as a model), and target DNA, respectively.

HCR has also been used in the construction of hemin/G-quadruplex DNAzyme amplifiers. For example, Yao's group[115] proposed a versatile strategy to construct DNAzyme hydrogel based on skillfully incorporating G-quadruplex DNAzyme sequences to the DNA motifs and HCR. The enzyme cascade could be activated through the integration of DNAzyme hydrogel with glucose oxidase(GOx) and β-galactosidase(β-gal). Their DNAzyme hydrogel could play the role of building blocks and biological units compared with previous enzyme cascade systems, which has better biocompatibility and an easier preparation process. Willner's group[69] constructed dye-loaded UiO-66 metal-organic framework nanoparticles(NMOFs) that were modified with hemin/G-quadruplex DNAzyme for the chemiluminescence resonance energy transfer(CRET) analysis of genes or miRNAs by combining HCR. As shown in Fig.6(B), the dye-loaded NMOFs are decorated with hairpin probes, which have recognition domains for the target nucleic acid and caged G-quadruplex segments. Targets could trigger HCR and the generation of chemiluminescence could be catalyzed by the self-assembly of hemin/G-quadruplex DNAzyme to stimulate CRET to the dye-loaded in the NMOFs to bring about the sensitive analysis of target genes and miRNAs.

Ding's group[116] proposed a dual amplification machine for the label-free ultrasensitive microRNA(miRNA) colorimetric biosensing, which is based on RCA and hemin/G-quadruplex DNAzyme. Li's group[117] constructed the hemin-bridged MOF with double amplification of RCA and G-quadruplex DNAzyme catalysis for the ultrasensitive lasting chemiluminescence imaging of microRNA. Tan's group[118] realized highly sensitive microRNA detection by combining hemin/G-quadruplex DNAzymes, nicking-enhanced RCA and MoS_2 quantum dots. In addition, Ju's group[70] combined RCA

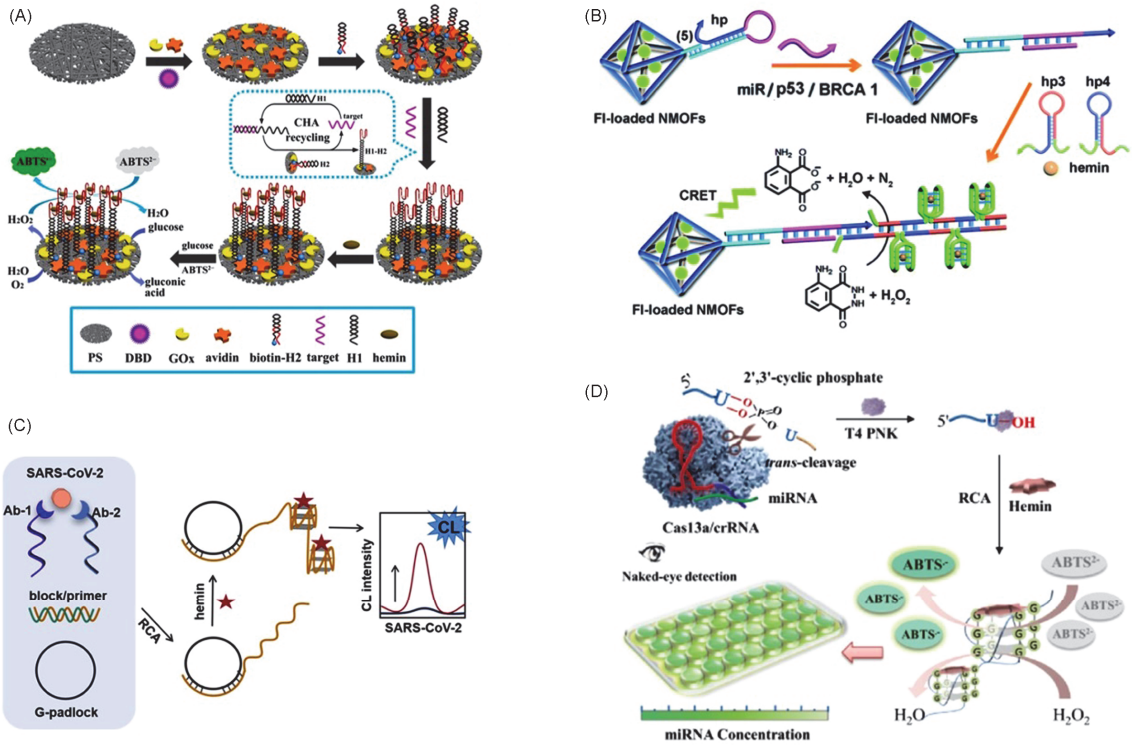

Fig.6 Schematic illustration of hemin/G-quadruplex DNAzyme signal amplification combined with other amplification methods (the formation of hemin/G-quadruplex DNAzyme could trigger peroxidation with ABTS and H_2O_2)

(A) CHA. Reprinted with permission from Ref.[114], Copyright 2016, Springer Nature; (B) HCR. Reprinted with permission from Ref.[69], Copyright 2021, The Royal Society of Chemistry; (C) RCA. Reprinted with permission from Ref.[70], Copyright 2021, American Chemical Society; (D) CRISPR/Cas13a-based signal amplification and RCA. Reprinted with permission from Ref.[119], Copyright 2021, American Chemical Society.

https://doi.org/10.1007/s40242-023-2334-8

with hemin/G-quadruplex DNAzyme in the purpose of chemiluminescence immunoassay of the SARS-CoV-2 protein. As shown in Fig.6(C), Ab-1/SARS-CoV-2/Ab-2 complex is formed by Ab-1 and Ab-2 conjugated through DNA-antibody. The complex including the complementary sequence of block DNA could recognize the target protein(SARS-CoV-2 protein) and thus make the primer release from the block/primer complex. Then the primer triggered RCA to form plentiful G-quadruplex DNAzyme units. In the existence of hemin, a remarkable chemiluminescent signal could be produced by hemin/G-quadruplex DNAzyme complex for the SARS-CoV-2 protein detection through luminol oxidation catalyzed by hydrogen peroxide. It is shown that a detectable concentration range was over 5 orders of magnitude by the work and the LOD was as low as 6.46 fg/mL.

In addition to enzyme-free methods, some proteins have become extensively used in the development of ultrasensitive biosensors. Xing's group[119] developed a CRISPR/Cas13a-based colorimetric system(vCas) for miR-10b visual detection with the LOD down to 1 fmol/L. As shown in Fig.6(D), in the presence of target miRNA, the uracil ribonucleotide(rU)-bearing pre-primer is cleaved collaterally by Cas13a/crRNA. Then the RCA process could be further stimulated by the remaining 5′-DNA fragment of pre-primer. The generated G-rich sequence could construct a tandem G-quadruplex, which binds to hemin to catalyze the oxidation of the $ABTS^{2-}$ and output visual color change. However, the complicated operation process of the vCas system limits its further application in clinical applications.

Besides $ABTS^{2-}$, the hemin/G-quadruplex DNAzyme structure could oxidize 3,3′,5,5′-tetramethylbenzidine(TMB) with H_2O_2. For example, Wang *et al*.[120] developed an amplification means for the target DNA detection, which is based on the target-induced construction of a three-way junction and it owns the LOD down to 0.8 pmol/L. In addition to simple strand hybridization reaction, Zhou *et al*.[121] proposed an enzyme-free and label-free colorimetric biosensor for Cd^{2+} detection with a detection limit down to 10 pmol/L, which realized the integration of split G-quadruplex DNAzymes, toehold-mediated strand displacement, and CHA.

3.4 DNAzyme-based Logic Gates

Biocomputing has attracted extensive interest in many fields for it shows great potential for multiparameter sensing applications, intelligent diagnostics, and advanced therapeutic. With the feature of being high programmable, DNAzymes have become extensively used in the fabrication of simple logic gates and digital computing circuits.

In most relevant studies, it is common to integrate multiple DNAzyme-based logic units to implement cascaded DNAzyme computing logic gate circuits[122]. One of the important performances of the computational circuit is to realize the signal transmission between different stages. Feedback is a special chemical mechanism that can realize the dynamic response of the system under different external conditions. For example, Levine's group[123] proposed a cascading logic system based on three Mg^{2+}-dependent DNAzymes that could generate third-order polynomial function. The logical system is divided into three layers. In each layer, the Mg^{2+} could catalyze DNAzyme to specifically cut a hairpin, and the output DNAzyme can be used as the input of the next layer. Feedback makes it easy for the concatenated automata to monitor the output, and even the output of each layer can be accurately measured.

In addition to applying DNAzyme-based digital computing circuits, researchers have also focused on how to transform DNAzyme-based logic gates into programmable, portable, reusable, and quantitative biosensing platforms. For example, Lu's group[124] developed a biocomputing platform that was based on a pocket-sized personal glucose meter(PGM) by utilizing nicotinamide adenine dinucleotide(NADH) and glucose as signal outputs. By designing a set of different logic gates(YES, NOT, INHIBIT, NOR, NAND, and OR), they had also successfully extended these biocomputing platforms to multiple biological substances, such as metal ions(Na^+), anions(citrate), disease-related native enzymes(alkaline phosphatase, pyruvate kinase, and alcohol dehydrogenases) and metabolites(adenosine diphosphate and adenosine triphosphate). These biocomputing platforms had also been proved to hold great potential in point-of-care(POC) diagnostics of diseases, such as hypernatremia and hyponatremia.

Besides, the construction of DNAzyme-based logic gates can realize real-time monitoring of the cell environment and develop intelligent diagnostic and treatment tools. However, the intracellular DNAzyme-based biological operation is greatly limited by the complex physiological environment and the low concentration of metal ions in the cell. In order to solve this problem, Chen *et al*.[125] proposed enzyme-powered DNAzyme nanodevices(DzNanos) through the programmed assembly of two logical units. As shown in Fig.7(A), they used MnO_2 nanosheets to promote the absorption of the whole system by the cells and provided cofactor Mn^{2+} for DNAzyme by the chemical reactions of the MnO_2 nanosheets in the cells to realize the logical operation of the DzNanos in living cells. In this interesting study, they further used cellular endogenous RNAs as the substrate to realize gene modulation for therapeutic applications. Lu's group[126] used Zn^{2+}- and Mg^{2+}-specific DNAzymes to build DNA switches ensuring two-factor control disassembly consisting of AND and OR

https://doi.org/10.1007/s40242-023-2334-8

operation for cell assembly and disassembly.

Peroxidase-mimicking hemin/G-quadruplex DNAzyme is an ideal signal sensor for the formation of functional DNA devices and DNA logic gates[127,128]. Chen's group[129] proposed a label-free and enzyme-free biosensor that used the caged G-quadruplex to construct a series of logic gates as the signal transducer. The hemin/G-quadruplex DNAzyme conformation could transform the output of these logic gates into visible color changes. As shown in Fig.7(B), it depicts how the exclusive OR(XOR) logic gate outputs a signal. Only in the presence of input 1(1, 0) or input 2(0, 1), the G-quadruplex DNAzyme sequence inside the cage would be released. Upon binding with hemin, the oxidation of TMB was catalyzed by the hemin/G-quadruplex DNAzyme structure with H_2O_2 to output a visible colored readout signal. Then they used this two-input modular design strategy to construct a series of other elementary logic gates. They even constructed two combinatorial gates by connecting two gates into a multilevel circuit. Liu's group[130] used a similar design strategy to construct a label-free and enzyme-free sensing platform for the ultrasensitive detection of Cd^{2+} with the LOD as low as 2.5 pmol/L. DNA nanodevices earlier mostly depended on strand displacement in the demand of oligodeoxynucleotides as inputs, which could lead to pollution in the whole system after a few switching cycles, thus lowering robustness and efficiency. As an external trigger, light can effectively eliminate the pollution caused by the introduction of oligodeoxynucleotides. Famulok's group[131] proposed a temporal and reversible light-controlled orthogonal photoswitching of G-quadruplex DNAzyme for complex biological operations. As shown in Fig.7(C), the whole system could reversibly and orthogonally control a 3:1 split G-quadruplex DNAzyme through applying four different wavelengths. The control of DNA hybridization was achieved by modifying the DNA strand with *N*-methyl-arylazopyrazole (AAP) and 2′,6′-dimethylazobenzene(DM-Azo). Time-dependent orthogonality was realized by the obvious difference in response time between DM-Azo and AAP to UV irradiation. They subsequently constructed a 4:2 multiplexer. The output was converted into two binary outputs by siting three different absorbance signa thresholds.

In other interesting studies, DNAzyme also has been used as a bridging device for nanomaterials to control the dissociation and assembly of nanoparticles or DNA origami to construct logic gates[132−134].

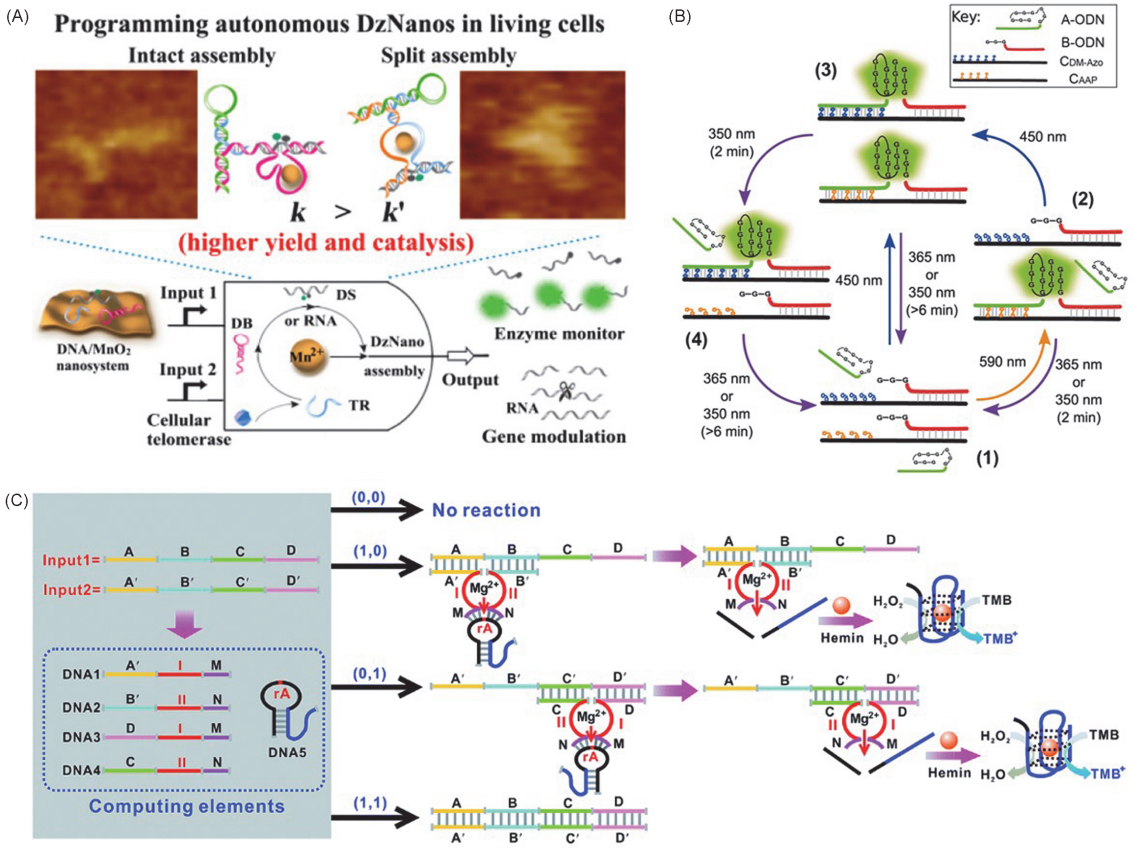

Fig.7 Schematic illustration of DNAzyme-based logic gates

(A) Enzyme-powered DNAzyme nanodevices(DzNanos) working in living cells. Reprinted with permission from Ref.[125], Copyright 2017, American Chemical Society; (B) G-quadruplex DNAzyme was used as the signal output element. Reprinted with permission from Ref.[129], Copyright 2018, The Royal Society of Chemistry; (C) temporal and reversible light-controlled orthogonal photoswitching of G-quadruplex DNAzyme for complex biological operations. Reprinted with permission from Ref.[131], Copyright 2018, American Chemical Society.

https://doi.org/10.1007/s40242-023-2334-8

3.5 DNAzyme-based Constitutional Dynamic Networks

The metabolism in cells is usually carried out by a complex dynamic chemical network. Under the stimulation of external conditions, the up-regulation and down-regulation can be realized. Researchers have devoted themselves to design assemblies imitating fundamental functions of biosystems and biomaterials to mimic complex cellular dynamic chemical networks[135−137].

The fabrication of constitutional dynamic networks(CDNs) is associated with the further improvement in the complexity of constitutional dynamic chemical systems. Among these systems, a series of macromolecular constituents or dynamical interconvertible molecular is produced. Under external chemical or physical stimuli, the entire network responds to the stimulus by adjusting its internal components. For example, Willner's group[138] proposed two different input-triggered DNAzyme-based CDNs with adaptive catalytic functions. As shown in Fig.8(A), it depicts the switchable reversible operations of the first CDN. A promoter nucleic acid played the role of controller and the T-A·T triplex motif played the role of regulator. The cleavage of the substrate modified with different fluorophores could produce different fluorescence, and the catalytic activity of different components in the mixed structure can be quantified according to the intensity of fluorescence. The initial content of different components could be evaluated by using the appropriate calibration curve. After that, they used a similar strategy that introduced the external effector strand to realize the orthogonal control of CDN. Although this DNAzyme-based CDN is composed of four constituents, Willner's group[139] further constructed [3×2] or [3×3] CDNs consisting of six or nine components. Subsequently, their group[140] constructed the three-dimensional CDNs, which were composed of eight three-component constituents. In principle, it is possible to design the CDNs to higher dimensionalities by introducing more other DNAzymes into the whole system.

Another important challenge is how to formulate a kinetic scheme to mimic the information interchange and component regulation between different CDNs. Willner's group[141] introduced the intercommunication between two CDNs. As shown in Fig.8(B), the two-CDN system is composed of two CDNs, "S" and "T". There were no common components and intercommunication between the two CDNs. Similar to the reported [2×2] CDN, both of the two CDNs composed of four equilibrated DNA nanostructures which could form activated Mg^{2+}-dependent DNAzyme. And another Mg^{2+}-dependent DNAzyme acted to interconnect the two networks as a functional catalytic activator unit. The construction of the

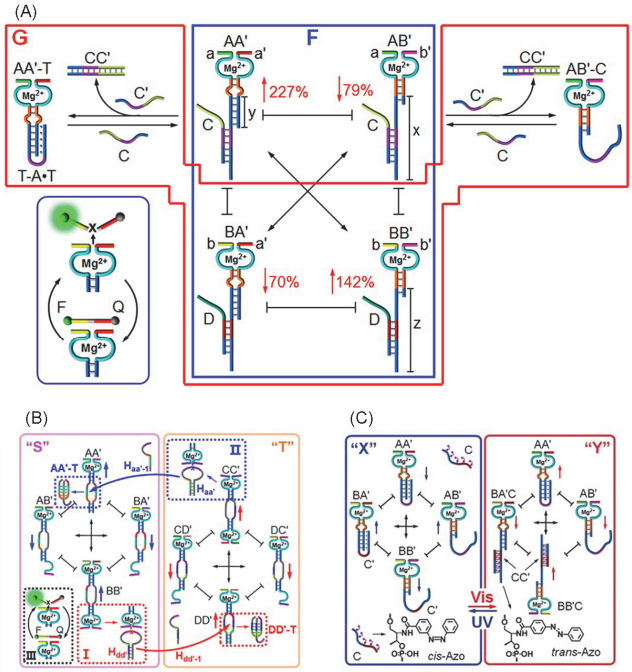

Fig.8 Schematic illustration of DNAzyme-based constitutional dynamic networks

(A) DNAzyme-based CDNs with adaptive catalytic functions. Reprinted with permission from Ref.[138], Copyright 2017, American Chemical Society; (B) intercommunication between two CDNs. Reprinted with permission from Ref.[141], Copyright 2018, American Chemical Society; (C) light-induced reversible switch of CDN. Reprinted with permission from Ref.[142], Copyright 2018, Wiley.

T-A·T triplex led to the stabilization of each equilibrated constituent and equilibrated CDN. Subsequently, they also realized orthogonal control of constituents. They proposed light-induced CDNs, which used an azobenzene-modified trigger strand[142]. The light-induced interconversion of conformations allowed the orthogonal control without added external oligonucleotide strands. As shown in Fig.8(C), through photoisomerization of azobenzene-modified strand C, the reversible switch of CDN "X" and "Y" was realized. Furthermore, they constructed another photoresponsive CDNs which realized switchable biological operations of the hemin/G-quadruplex DNAzyme.

4 Biological Applications of DNAzyme-based Nanodevices

DNAzymes have drawn much attention owning to their inherent specific recognition and catalytic properties[143−146]. DNAzyme-based nanodevices are widely used in many biological applications due to their various excellent properties. For example, the thermal and buffer stability of the DNAzymes make it an excellent alternative to protein enzymes to identify the targets. In addition, by designing the different binding sequences to be complementary to target

https://doi.org/10.1007/s40242-023-2334-8

mRNAs, DNAzymes can efficiently and specifically cleave target mRNAs. In this section, we introduce the application of DNAzyme-based nanodevices in therapy and biosensing.

4.1 Biosensing

4.1.1 Metal Ions

Heavy metal ions, a great threat to animals and humans, are one of the main pollutants in natural environment. Recently, a lot of DNAzyme-based strategies for detecting heavy metal ions *in vitro* have been realized[31,43,147]. For example, Chen's group[148] proposed a convenient transducer for the detection of Pb^{2+}, which combined the advantages of specific catalytic properties of DNAzyme, the high accuracy, and easy access to electronic balance.

Celluar endogenous metal ions play a vital role in cell metabolism and pathological processes. In order to further explore the relationship between intracellular biological processes and endogenous metal ions, it is necessary to monitor the concentration and location of metal ions in cells. Various nanoparticles were commonly used as carriers to improve the efficiency of DNAzyme probes uptaken by cells, such as graphene oxide(GO)[149], upconversion nanoparticles (UCNPs)[150], and gold nanoparticles[151,152]. On the other hand, these nanocarriers can effectively improve the resistance of DNAzyme probes to the nuclease, which realizes potential applications in the complex physiological environment.

Toward realizing high spatial and temporal resolution imaging of intracellular metal ions, many people have made numerous efforts to develop different imaging strategies. Currently, most reported DNAzyme-based fluorescence biosensors are modified with one-photon fluorophores with shallow tissue penetration depth(<100 μm). To solve this problem, a DNAzyme-based two-photon(TP) imaging probe (TP-8-17ES-AuNP) was proposed for Zn^{2+} detection inside living cells by Zhang's group[151]. As shown in Fig.9(A), both the quencher and AuNPs can quench the TP fluorophore. The TP fluorophore-labeled substrate strand could be cleaved only in the presence of Zn^{2+} by the DNAzyme, producing fluorescence signal and realizing TP imaging. This two-photon probe successfully imaged Zn^{2+} with a tissue penetration as high as 160 μm. In addition, Lu's group[150] proposed a DNAzyme-based near-infrared(NIR) probe in larvae of zebrafish and early embryos for real-time metal ion tracking with spatiotemporal control. In order to overcome the limitations of 365 nm light's inability to penetrate tissue and its strong phototoxicity, they conjugated the photocaged DNAzyme probe to a UCNP(NaYF4:Yb, Tm@NaYF4), which could transfer 980-nm excitation into 365-nm emission. After 980-nm irradiation, the photocaged molecule would be photodissociated from the substrate strand and exposed to the cleavage site. However, the use of the external light stimulus control sensor still has many disadvantages, such as insufficient light penetration depth and potential biotoxicity from high doses of radiation. Lu's group[153] further proposed another biosensor that could bio-orthogonal control of imaging endogenous metal ions by using a homing endonuclease I-SceI enzyme to activate the 10-23 DNAzyme in living cells.

Compared with organic fluorescent dyes, fluorescent proteins have many advantages as a signal reporter, such as excellent photostability and biocompatibility. Zhang's group[154] designed a method for ratiometric imaging of metal ions and metal ion detection in living systems, which is based on the combination of genetically encoded fluorescent proteins and 10-23 DNAzyme. As shown in Fig.9(B), red fluorescent protein mutant Ruby2 and green fluorescent protein mutant Clover2 were selected as a permanent reference and a signal reporter, respectively, for ratiometric measurement, named as CloverFP and RubyFP. In the existence of target metal ions, the RNA-cleaving 10-23 DNAzymes could specifically cleave the mRNA transcripts for CloverFP, resulting in down-regulation of CloverFP, while the same DNAzyme will not affect the expression of RubyFP. Our method shows the advantage of Mg^{2+}-dependent multi-turnover cleavage, which makes fluorescent protein expression level correlated with the concentration of intracellular metal ions.

4.1.2 Non-metal Targets

Intracellular MicroRNAs(miRNAs) are a kind of non-coding single-strand RNA molecules(18—25 nucleotides), which play an important role in a variety of physiological processes. Many studies have revealed the potential of miRNAs as biomarkers for a range of diseases, such as diabetes, cardiovascular diseases, and cancer. The quantitative and imaging of RNAs in living cells has become increasingly important for understanding intracellular RNA dynamics with spatiotemporal resolution. In recent years, a series of DNAzyme-based fluorescence sensors has been developed for the quantitative detection of miRNAs in cells[90,155—157]. At the same time, direct imaging of low-abundance endogenous miRNAs would provide a valuable tool for estimating the drug efficiency and monitoring the pathological microenvironments of cancers in real time. Chu's group[90] proposed a DNAzyme-based walker to realize the miRNAs imaging in living cells. However, due to the long operating time(180 min) of the above walking machine, their group has introduced a PC linker to design a photocontrolled bipedal DNA walker for intracellular miRNA imaging[91].

To overcome the low abundance of miRNAs, researchers

developed a series of amplification strategies to realize the ultrasensitive miRNAs imaging in living cells[90,108,117,158,159]. Chu's group[158] proposed an enzymatic RCA strategy in living cells for endogenous miRNAs imaging. They used the pH-sensitive biodegradable metal-organic framework nanoparticles(MOF NPs) of zeolitic imidazolate framework-8 (ZIF-8) to co-deliver nucleic acid probes and phi29 polymerase(ϕ29DP). The MOF NPs would dissociate in the endolysosomes and release cargoes. The endogenous miRNAs triggered RCA reaction and the synthesized DNAzyme would cleave the substrate, which was modified with fluorophore/quencher pair, realizing the ultrasensitive miRNA imaging in living cells. Li's group[117] also employed MOF as a functional interface to construct the double-amplified chemiluminescence(CL) sensing platform for microRNA imaging. Moreover, Zhang's group[160] proposed a stimuli-responsive nanosystem containing Cu-MOF and DNAzyme-based signal amplification for imaging of aberrant miRNA.

As the main energy carrier in many physiological systems, ATP can be stored as energy in living cells or be transformed to ADP and release energy, which can regulate diverse cell life activities. Many studies have proved that anomalous variation of ATP concentration is related to many diseases. Herein, the development of highly sensitive and accurate detection methods of ATP is of great significance for clinical diagnosis and treatment. Xiang's group[161] designed a label-free and non-enzymatic means for dual amplified detection of ATP in human serums. Wang's group[162] proposed an aptazyme sensor for the amplified detection in living cells with a detection limit as low as about 200 nmol/L. Subsequently, Li's group[21] used a self-phosphorylating DNAzyme(SPDz) for rapid and specific imaging of ATP. As shown in Fig.9(C), they modified fluorescently labeled DK1(^{F}DK1) with cholesterol at the 3′ end to form the SPDz sensor, which could anchor on the cell surface. In the existence of ATP, ^{F}DK1 will convert a phosphate group from ATP to its 5′ end in self-phosphorylation reaction buffer(SPB). Exonuclease reaction buffer could stop the phosphorylation reaction and ^{F}DK1 could bind to ^{Q}DO to cause fluorescence quenching. Besides, λ-exo could catalyze the removal of 5′ mononucleotides from the 5′-phosphorylated ^{F}DK1-^{Q}DO complex to produce a strong fluorescence signal, enabling the detection concentration of ATP as low as 3 μmol/L and fluorescence imaging of extracellular ATP transients at the single-cell level with high specificity that occur in the subsecond time range.

Amino acids are the basic substances of protein required by animal nutrition and play an important role in biological metabolism. Fu *et al*.[163] constructed a DNA cage molecular sieve-based DNAzyme probe for intracellular biosensing of *L*-histidine(*L*-His), a conditionally essential amino acid. As shown in Fig.9(D), *L*-His DNAzyme with quencher(DABCYL) was composed into the cavity of DNA cage molecular sieve, quenching the fluorophore(FAM) labeled on the substrate strand. Only in the existence of the target *L*-His, the DNAzyme could cleave the substrate strand to trigger the recovery of fluorescence signal. Importantly, the DNA cage can avoid contact between DNAzyme and macromolecules, such as proteins and nucleases, thus protecting the DNAzyme from nonspecific protein binding and rapid nuclease degradation. Moreover, Xu's group[164] designed a simple, disposable

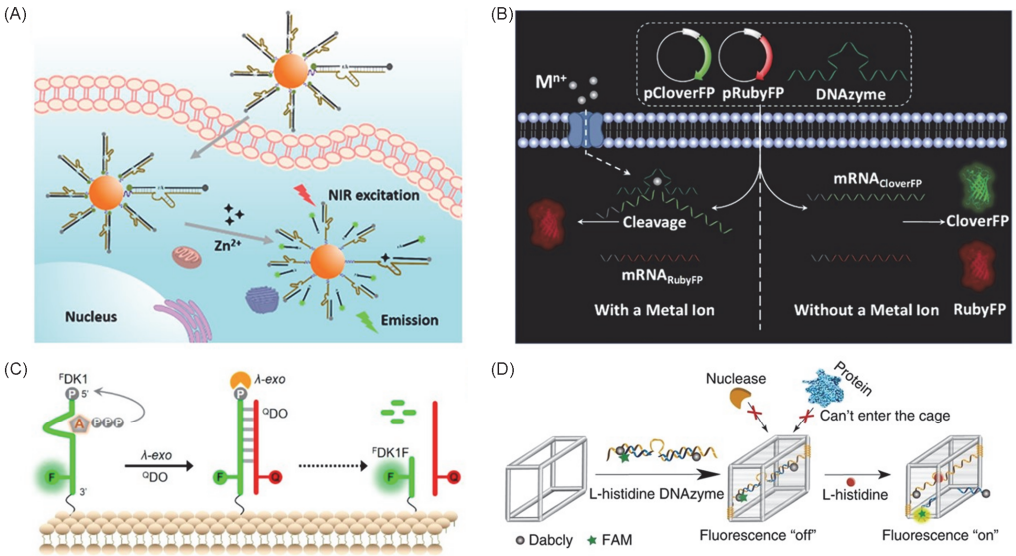

Fig.9 Schematic illustration of the applications of DNAzyme-based nanodevices in biosensing

Metal ion targets: (A) a DNAzyme-based two-photon imaging probe for the detection of Zn^{2+} in living cells. Reprinted with permission from Ref.[151], Copyright 2018, American Chemical Society; (B) a ratiometric imaging strategy of metal ions in living systems based on 10-23 DNAzyme. Reprinted with permission from Ref.[154], Copyright 2020, Wiley; non-metal targets: (C) a self-phosphorylating DNAzyme(SPDz) for rapid and specific imaging of ATP. Reprinted with permission from Ref.[21], Copyright 2021, American Chemical Society; (D) a protective confined-based DNAzyme probe for *L*-His biosensing. Reprinted with permission from Ref.[163], Copyright 2020, Springer Nature.

https://doi.org/10.1007/s40242-023-2334-8

electrochemical nanotool for the quantification of cytoplasmic *L*-His integrating the nanopipette and *L*-His DNAzyme.

In addition to imaging miRNAs, ATP and amino acids, DNAzymes have also been used for imaging other macromolecules, such as proteins. Proteins are a type of organic macromolecules, which are the basic organic substances of cells. Proteins play an important role in various biochemical reactions. The significant impacts have attracted researchers' attention to the detection of proteins using DNAzyme-based devices, such as thrombin[84,85,165], antibodies[166−169], telomerase[170], and some other proteins[26,94,110,171−174].

4.2 Therapy

Over the past few years, DNAzymes-based therapeutic nanodevices are particularly attractive due to their highly biocompatible, excellent specificity, and low cost. The biggest advantage of DNAzymes for theranostics probably is the highly programmable feature adapted to different diseases[175−177]. DNAzymes-based therapeutic nanodevices can identify different targets through designing two arms, which is more difficult for nanomaterials. Therefore, it is quite potential to rationally design DNAzymes-based nanodevices for therapeutic applications.

For now, the therapeutic applications of DNAzymes fall into two broad categories. Firstly, DNAzymes can perform as "molecular gatekeepers" to control stimuli-responsive drug release. Secondly, the inherent catalytic-cleavage characteristic makes DNAzymes act as an excellent tool for gene silencing. The cleavage of HIV-1 integrase gene with 10-23 DNAzymes downregulated 70%—80% of HIV integrase protein, which efficiently inhibited the integration of the HIV-1 genome into the host DNA[178]. Further research shows that the gene silencing efficiency of DNAzymes in tumor therapy is up to 40%[175]. With the rapid development of nanomaterials, a series of nanoplatforms is widely used to solve the problems of traditional chemotherapy. Accordingly, researchers also have developed multifunctional theranostic platforms, which combine DNAzymes with nanomaterials.

To realize stimuli-responsive drug release, Shi's group[179] proposed Mg^{2+}-dependent DNAzyme functionalized hollow mesoporous magnesium silicate nanoparticles(HMMSNs) loading with an anticancer drug(doxorubicin, DOX). The biodegradation of HMMSNs in the mild acidic tumor-associated microenvironment could offer Mg^{2+} to trigger the release of DOX. To further overcome the nontargeted cytotoxicity and accumulation of exogenous nanomaterials, endogenously generated biomaterials have attracted extensive attention for biomedical research. Wang's group[23] fabricated ZnO-encapsulated DNAzyme nanosponges(NSs) for stimuli-responsive drug release and self-sufficient cancer therapy. They further integrated therapeutic DNAzyme and self-catabolic DNAzyme to construct a bioinspired self-degradable multifunctional DNAzyme nanosponge for programmable delivery of drugs and realizing an efficient DNAzyme-mediated gene silencing on targeted cancer cells[24].

In addition to traditional chemotherapy, gene therapy(GT) can also achieve the purpose of triggering cancer cells apoptosis or necrosis by destroying genetic material(DNA or RNA)[180,181]. Despite decades of effort, GT still failed to achieve a breakthrough in clinical application due to low selectivity, unsatisfactory sensitivity, and off-target effect. To address the aforementioned problems, Kolpashchikov's group[182] proposed a DNAzyme-based nanodevice that cleaved the mRNA of a housekeeping gene. However, RNA-cleaving deoxyribozymes-based GT still exists some disadvantages, such as unsatisfactory intracellular delivery efficiency. To solve this problem, Ahn's group[183] designed a DNAzyme-based tetrahedral wireframe to enhance gene-silencing activity and cellular uptake efficiency. In addition to tetrahedral wireframe, tetrahedral DNA nanostructures(TDNs) have also been used to deliver therapeutic DNAzymes[184]. Chaput's group[27] made an effort to silencing gene by RNA-cleaving DNAzymes to overcome their low therapeutic applications efficiency in clinical trials. As shown in Fig.10(A), they have constructed promising modified 10-23 DNAzyme by introducing nucleotide mimics(2′-fluoroarabino nucleic acid and α-l-threofuranosyl nucleic acid backbone architectures) to form a new DNAzyme reagent X10-23, which exhibited even higher gene-silencing activity than the corresponding antisense oligonucleotides in mammalian cells.

Besides DNA nanostructure-based carriers, inorganic nanocarriers can also be used to transport therapeutic DNAzymes into cells. The synergy therapy can be realized by adding photosensitizer(PS) or photothermal agents(PTAs) into inorganic nanomaterials, such as MnO_2 nanomaterials[185,186], Cu(tz) nanosheet[187], metal-organic frameworks(MOFs)[25], and upconversion nanoparticles(UCNPs)[188].

Photodynamic therapy(PDT) employs PS to produce singlet oxygen(SO) and reactive oxygen species(ROS) to realize DNA damage and cell apoptosis with light irradiation[189−192]. Tan's group[185] proposed a DNAzyme-MnO_2 nanodevice for synergistic therapy involving PDT and GT. As shown in Fig.10(B), the chlorin e6-labeled DNAzymes(Ce6) were adsorbed on MnO_2 nanosheets by physisorption. MnO_2 nanosheets have multi-purpose, both nanocarrier of the DNA, and cofactor(Mn^{2+}) provider for activating 10-23 DNAzyme, an activatable MRI contrast agent, and a quencher for the generation and fluorescence of singlet oxygen from Ce6. Chu's group[186] also used a similar strategy to design a DNAzyme-MnO_2 nanodevice for telomerase-triggered cancer

cell therapy. Chen's group[187] used Cu(I) 1,2,4-triazolate nanoscale coordination polymers nanosheets, which could act as both an intrinsic photosensitizer for hypoxia-tolerant type I PDT and an effective DNAzyme nanocarrier for GT.

Photothermal therapy(PTT) employs PTAs to generate heat from near-infrared(NIR) light absorption, resulting in thermal ablation of cancer cells[193,194]. Wang's group[195] proposed polydopamine Mn^{2+} nanoparticles(MnPDAs) with multiple functions besides effective DNAzyme delivery nanocarrier, enabled synergetic GT, PTT, and multimodal imaging. Based on similar strategies, Yang's group[29] combined RCA to build a synergistic DNA-polydopamine-MnO_2 nanocomplex enabling NIR-light-powered catalytic activity of DNAzyme *in vivo*. As shown in Fig.10(C), RCA could generate DNA nanoframework containing repeated DNAzyme sequences as scaffolds to bind polydopamine-MnO_2(PM) to form DNA-polydopamine-MnO_2 nanocomplex. In the tumor microenvironment, GSH can degrade PM and release Mn^{2+} to initiate DNAzyme for gene regulation. Meanwhile, upon NIR-light radiation, polydopamine can produce the photothermal effect at the tumor site to achieve PTT.

Chemodynamic therapy(CDT) is an emerging therapeutic assay that uses Fenton reaction mediated by Fe^{2+} or Fenton-like reaction mediated by Cu^{2+} or Mn^{2+} to convert hydrogen peroxide(H_2O_2) in tumor sites into the harmful hydroxyl radical(·OH) of reactive oxygen species(ROS) to induce cell apoptosis[196−198]. There are several examples of combining DNAzyme with CDT. Zhao's group[199] combined DNAzymes-loaded zeolitic imidazolate frameworks(ZIFs@Dz) with ferrous cysteine-phosphotungstate(FeCysPW) to form a nanoplatform FeCysPW@ZIF-82@CATDz, which could disrupt tumor break redox homeostasis(RHD) to improve ROS-mediated CDT, which also promotes GT. However, Fe^{2+}-catalyzed Fenton reaction for CDT is only efficient in highly acidic environments(pH 2—4), which shows relatively low efficiency to eliminate cancer cells. To overcome this problem, Zhao's group[200] designed a simple approach to forming Cu-DNAzyme nanohybrids for CDT and GT. As shown in Fig.10(D), DNAzyme and Cu^{2+} were co-assembled through coordination interactions to form a single nanoparticle (Cu-Dzy). Subsequently, a thin layer of metal-phenolic networks was coated to form the final therapeutic agent Cu-Dzy@TA, which could release DNAzyme in cancer cells for silencing target mRNA to achieve GT. Meanwhile, Cu^{2+} could consume GSH in cancer cells and be reduced to Cu^{+} to catalyze H_2O_2 to produce ·OH to achieve efficient CDT.

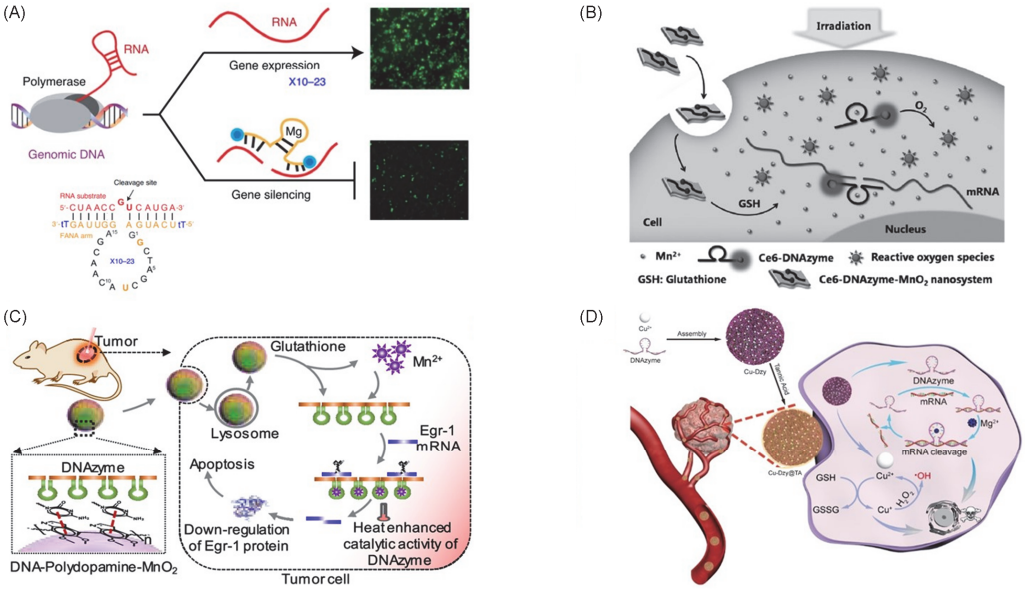

Fig.10 Schematic illustration of the applications of DNAzyme-based nanodevices in therapy

(A) X10-23 DNAzyme for gene-silencing in mammalian cells enabling GT. Reprinted with permission from Ref.[27], Copyright 2021, Springer Nature; (B) a DNAzyme-MnO_2 nanodevice for synergistic therapy involving PDT and GT. Reprinted with permission from Ref.[185], Copyright 2015, Wiley; (C) DNA-polydopamine-MnO_2 nanocomplex enabled synergetic PTT and GT. Reprinted with permission from Ref.[29], Copyright 2021, American Chemical Society; (D) therapeutic agent Cu-Dzy@TA for CDT and GT. Reprinted with permission from Ref.[200], Copyright 2021, Wiley.

5 Summary and Outlook

In this review, we summarized the applications of DNAzyme-based nanodevices in biosensing and therapy. DNAzymes are obtained by selection *in vitro* and exhibit the advantages of easy modification and functionalization, remarkable specificity toward cofactors, and the excellent catalytic activity. Thus, much efforts are made on the construction and biological applications of DNAzyme-based nanodevices,

https://doi.org/10.1007/s40242-023-2334-8

such as DNA walkers, DNA tweezers, signal amplifiers, logic gates, and constitutional dynamic networks. Although many achievements have been obtained in recent years, there are still some challenges worth taking.

First, specifically catalytic mechanism is still not clear. The catalytic activity of DNAzymes depends on the construction of well-defined secondary or tertiary structures, in this connection, more structural biology data are needed to explore the mechanism. Clarifying the catalytic cleavage mechanism will be useful for the development of *in vitro* screening techniques. New selection methods could bring in new DNAzymes which can catalyze more diverse kinds of chemical reactions, so as to widen the scope of application.

Second, their sensing and therapeutic performance in living cells and living bodies is in urgent need of improvement. Complex physiological environment may introduce a large number of false positive signals. An existing strategy is to insert photocaged groups(such as nitrobenzyl) on ribonucleotide cleavage sites to realize photo-controllable biological applications. However, the typical decaying time of the most commonly used nitrobenzyl group is up to 30 min and the process of lifting the blockade is essentially irreversible. Therefore, it is urgent to develop new caging strategies to overcome the above problems.

Third, DNAzyme probes in specific organelles cannot be located accurately. These organelles, such as Golgi apparatus and endoplasmic reticulum, play an important role in the physiological process, and the detection of targets in specific organelles is of great significance in the study of physiological processes. We believe that this problem can be solved by combining DNAzyme-based probes with targeted ligands, such as aptamers.

Furthermore, there are very few DNAzyme-based computing systems running in living bodies. Although DNA computation that relies on the programmed and automation operation of DNAzyme-based nanodevices is emerging, the accuracy of this system in living bodies is limited to the complicated physiological environment. We look forward to seeing further advancements in this field that can provide a potential platform for *in vivo* precision medicine.

Finally, the development of DNAzymes as drugs remains in their early infancy. In the near future, these agents may become practical and economical anti-cancer therapies. But for now, the therapeutic application of DNAzymes needs further study, particularly in clinical tests, and the biosafety of DNAzyme-based nanodevices working in living cells need more rigorous tests. With these improvements, DNAzyme-based nanodevices are expected to play more and more important roles in the fields of bioanalysis and biomedicine[201−205].

Acknowledgements

This work was supported by the National Natural Science Foundation of China (Nos.22122403, 22274042, and 21890744), the Natural Science Foundation of Hunan Province, China(Nos.2021JJ10012, 2022JJ30121) and the Changsha Municipal Natural Science Foundation, China(No.kq2202145).

Conflicts of Interest

The authors declare no conflicts of interest.

References

[1] Di Z., Zhao J., Chu H., Xue W., Zhao Y., Li L., *Adv. Mater.*, **2019**, *31*, e1901885
[2] Shi H., Wang Y., Zheng J., Ning L., Huang Y., Sheng A., Chen T., Xiang Y., Zhu X., Li G., *ACS Nano*, **2019**, *13*, 12840
[3] Wang X., Kim G., Chu J. L., Song T., Yang Z., Guo W., Shao X., Oelze M. L., Li K. C., Lu Y., *J. Am. Chem. Soc.*, **2022**, *144*, 5812
[4] Wang Z., Song L., Liu Q., Tian R., Shang Y., Liu F., Liu S., Zhao S., Han Z., Sun J., Jiang Q., Ding B., *Angew. Chem. Int. Ed.*, **2021**, *60*, 2594
[5] Molden T. A., Niccum C. T., Kolpashchikov D. M., *Angew. Chem. Int. Ed.*, **2020**, *59*, 21190
[6] Liu S., Jiang Q., Zhao X., Zhao R., Wang Y., Wang Y., Liu J., Shang Y., Zhao S., Wu T., Zhang Y., Nie G., Ding B., *Nat. Mater.*, **2021**, *20*, 421
[7] Yue L., Wang S., Zhou Z., Willner I., *J. Am. Chem. Soc.*, **2020**, *142*, 21577
[8] Deng J., Liu W., Sun M., Walther A., *Angew. Chem. Int. Ed.*, **2022**, *61*, e202113477
[9] Du Y., Peng P., Li T., *ACS Nano*, **2019**, *13*, 5778
[10] Zhang Q., Xia K., Jiang M., Li Q., Chen W., Han M., Li W., Ke R., Wang F., Zhao Y., Liu Y., Fan C., Gu H., *Angew. Chem. Int. Ed.*, **2022**, e202212011
[11] Ellington A. D., Szostak J. W., *Nature*, **1990**, *346*, 818
[12] Beaudry A. A., Joyce G. F., *Science*, **1992**, *257*, 635
[13] Liu J., Cao Z., Lu Y., *Chem. Rev.*, **2009**, *109*, 1948
[14] Breaker R. R., Joyce G. F., *Chem. Bio.*, **1994**, *1*, 223
[15] Lu L. M., Zhang X. B., Kong R. M., Yang B., Tan W., *J. Am. Chem. Soc.*, **2011**, *133*, 11686
[16] Santoro S. W., Joyce G. F., Sakthivel K., Gramatikova S., Barbas C. F., *J. Am. Chem. Soc.*, **2000**, *122*, 2433
[17] Santoro S. W., Joyce G. F., *Proc. Natl. Acad. Sci. USA*, **1997**, *94*, 4262
[18] Li J., Zheng W., Kwon A. H., Lu Y., *Nucleic Acids Res.*, **2000**, *28*, 481
[19] Zhang X. B., Wang Z., Xing H., Xiang Y., Lu Y., *Anal. Chem.*, **2010**, *82*, 5005
[20] Elbaz J., Shlyahovsky B., Willner I., *Chem. Comm.*, **2008**, *13*, 1569
[21] Zhao D., Chang D., Zhang Q., Chang Y., Liu B., Sun C., Li Z., Dong C., Liu M., Li Y., *J. Am. Chem. Soc.*, **2021**, *143*, 15084
[22] Yang Y., Zhu W., Feng L., Chao Y., Yi X., Dong Z., Yang K., Tan W., Liu Z., Chen M., *Nano Lett.*, **2018**, *18*, 6867
[23] Wang J., Wang H., Wang H., He S., Li R., Deng Z., Liu X., Wang F., *ACS Nano*, **2019**, *13*, 5852
[24] Wang J., Yu S., Wu Q., Gong X., He S., Shang J., Liu X., Wang F., *Angew. Chem. Int. Ed.*, **2021**, *60*, 10766
[25] Wang H., Chen Y., Wang H., Liu X., Zhou X., Wang F., *Angew. Chem. Int. Ed.*, **2019**, *58*, 7380
[26] Wang Q., Tan K., Wang H., Shang J., Wan Y., Liu X., Weng X., Wang F., *J. Am. Chem. Soc.*, **2021**, *143*, 6895
[27] Wang Y., Nguyen K., Spitale R. C., Chaput J. C., *Nat. Chem.*, **2021**, *13*, 319
[28] Wang Z., Niu J., Zhao C., Wang X., Ren J., Qu X., *Angew. Chem. Int. Ed.*, **2021**, *60*, 12431
[29] Zhao H., Zhang Z., Zuo D., Li L., Li F., Yang D., *Nano Lett.*, **2021**, *21*, 5377
[30] Carmi N., Balkhi S. R., Breaker R. R., *Proc. Natl. Acad. Sci. USA*, **1998**, *95*, 2233
[31] Purtha W. E., Coppins R. L., Smalley M. K., Silverman S. K., *J. Am. Chem. Soc.*, **2005**, *127*, 13124
[32] Lu C. H., Wang F., Willner I., *J. Am. Chem. Soc.*, **2012**, *134*, 10651
[33] Cuenoud B., Szostak J. W., *Nature*, **1995**, *375*, 611
[34] Li Y., Breaker R. R., *Proc. Natl. Acad. Sci. USA*, **1999**, *96*, 2746
[35] Chandrasekar J., Silverman S. K., *Proc. Natl. Acad. Sci. USA*, **2013**, *110*, 5315
[36] Camden A. J., Walsh S. M., Suk S. H., Silverman S. K., *Biochemistry*, **2016**, *55*, 2671
[37] Lyu M., Kong L., Yang Z., Wu Y., McGhee C. E., Lu Y., *J. Am. Chem. Soc.*, **2021**, *143*, 9724
[38] Zimmermann A. C., White I. M., Kahn J. D., *Talanta*, **2020**, *211*, 120709
[39] Jimenez R. M., Polanco J. A., Luptak A., *Trends Biochem. Sci.*, **2015**, *40*, 648

[40] Santoro S. W., Joyce G. F., *Biochemistry*, **1998**, *37*, 13330
[41] Schubert S., Gul D. C., Grunert H. P., Zeichhardt H., Erdmann V. A., Kurreck J., *Nucleic Acids Res.*, **2003**, *31*, 5982
[42] Breaker R. R., Joyce G. F., *Chem. Bio.*, **1995**, *2*, 655
[43] Li J., Lu Y., *J. Am. Chem. Soc.*, **2000**, *122*, 10466
[44] Torabi S. F., Wu P., McGhee C. E., Chen L., Hwang K., Zheng N., Cheng J., Lu Y., *Proc. Natl. Acad. Sci. USA*, **2015**, *112*, 5903
[45] Zhou W., Zhang Y., Huang P. J., Ding J., Liu J., *Nucleic Acids Res.*, **2016**, *44*, 354
[46] Gellert M., Lipsett M. N., Davies D. R., *Proc. Natl. Acad. Sci. USA*, **1962**, *48*, 2013
[47] Kosman J., Juskowiak B., *Anal. Chim. Acta*, **2011**, *707*, 7
[48] Li Y., Sen D., *Biochemistry*, **1997**, *36*, 5589
[49] Travascio P., Li Y., Sen D., *Chem. Biol.*, **1998**, *5*, 505
[50] Gong L., Zhao Z., Lv Y. F., Huan S. Y., Fu T., Zhang X. B., Shen G. L., Yu R. Q., *Chem. Comm.*, **2015**, *51*, 979
[51] Stadlbauer P., Islam B., Otyepka M., Chen J., Monchaud D., Zhou J., Mergny J.-L., Šponer J., *J. Chem. Theory Comput.*, **2021**, *17*, 1883
[52] Cheng X., Liu X., Bing T., Cao Z., Shangguan D., *Biochemistry*, **2009**, *48*, 7817
[53] Kong D. M., Wu J., Wang N., Yang W., Shen H. X., *Talanta*, **2009**, *80*, 459
[54] Kong D. M., Yang W., Wu J., Li C. X., Shen H. X., *Analyst*, **2010**, *135*, 321
[55] Kong D. M., Xu J., Shen H. X., *Anal. Chem.*, **2010**, *82*, 6148
[56] Stefan L., Denat F., Monchaud D., *Nucleic Acids Res.*, **2012**, *40*, 8759
[57] Stefan L., Denat F., Monchaud D., *J. Am. Chem. Soc.*, **2011**, *133*, 20405
[58] Qi C., Zhang N., Yan J. L., Liu X. J., Bing T., Mei H. C., Shangguan D. H., *RSC Adv.*, **2014**, *4*, 1441
[59] Li W., Li Y., Liu Z., Lin B., Yi H., Xu F., Nie Z., Yao S., *Nucleic Acids Res.*, **2016**, *44*, 7373
[60] Albada H. B., Golub E., Willner I., *Chem. Sci.*, **2016**, *7*, 3092
[61] Wang Z. G., Wang H., Liu Q., Duan F. Y., Shi X. H., Ding B. Q., *ACS Catal.*, **2018**, *8*, 7016
[62] Xiao L., Zhou Z., Feng M., Tong A., Xiang Y., *Bioconjug. Chem.*, **2016**, *27*, 621
[63] Xiao Y., Pavlov V., Gill R., Bourenko T., Willner I., *Chembiochem*, **2004**, *5*, 374
[64] Wang D., Chai Y., Yuan Y., Yuan R., *Anal. Chem.*, **2019**, *91*, 3561
[65] Shen P., Li W., Liu Y., Ding Z., Deng Y., Zhu X., Jin Y., Li Y., Li J., Zheng T., *Anal. Chem.*, **2017**, *89*, 11862
[66] Ge C., Luo Q., Wang D., Zhao S., Liang X., Yu L., Xing X., Zeng L., *Anal. Chem.*, **2014**, *86*, 6387
[67] Huang R., He L., Xia Y., Xu H., Liu C., Xie H., Wang S., Peng L., Liu Y., Liu Y., He N., Li Z., *Small*, **2019**, *15*, e1900735
[68] Hu Z., Yang J., Xu F., Sun G., Pan X., Xia M., Zhang S., Zhang X., *J. Am. Chem. Soc.*, **2021**, *143*, 12361
[69] Zhang P., Ouyang Y., Willner I., *Chem. Sci.*, **2021**, *12*, 4810
[70] Zhang R., Wu J., Ao H., Fu J., Qiao B., Wu Q., Ju H., *Anal. Chem.*, **2021**, *93*, 9933
[71] Zhu L., Ye J., Yan M., Yu L., Peng Y., Huang J., Yang X., *Anal. Chem.*, **2021**, *93*, 2644
[72] Shin J. S., Pierce N. A., *J. Am. Chem. Soc.*, **2004**, *126*, 10834
[73] Tian Y., He Y., Chen Y., Yin P., Mao C., *Angew. Chem. Int. Ed.*, **2005**, *44*, 4355
[74] Cha T. G., Pan J., Chen H., Salgado J., Li X., Mao C., Choi J. H., *Nat. Nanotechnol.*, **2014**, *9*, 39
[75] Chen J., Luo Z., Sun C., Huang Z., Zhou C., Yin S., Duan Y., Li Y., *Trends Analyt. Chem.*, **2019**, *120*, 115626
[76] Liu X., Niazov-Elkan A., Wang F., Willner I., *Nano Lett.*, **2013**, *13*, 219
[77] Zhu L., Liu Q., Yang B., Ju H., Lei J., *Anal. Chem.*, **2018**, *90*, 6357
[78] He J. L., Zhang Y., Mei T. T., Tang L., Huang S. Y., Cao Z., *Biosens. Bioelectron.*, **2019**, *144*, 111692
[79] Chai H., Wang M., Zhang C., Tang Y., Miao P., *Bioconjug. Chem.*, **2020**, *31*, 764
[80] Ge J., Zhao Y., Gao X., Li H., Jie G., *Anal. Chem.*, **2019**, *91*, 14117
[81] Yang X., Shi D., Zhu S., Wang B., Zhang X., Wang G., *ACS Sens.*, **2018**, *3*, 1368
[82] Cai S., Chen M., Liu M., He W., Liu Z., Wu D., Xia Y., Yang H., Chen J., *Biosens. Bioelectron.*, **2016**, *85*, 184
[83] Qing M., Xie S., Cai W., Tang D., Tang Y., Zhang J., Yuan R., *Anal. Chem.*, **2018**, *90*, 11439
[84] Xiong E., Zhen D., Jiang L., Zhou X., *Anal. Chem.*, **2019**, *91*, 15317
[85] Du H., Yang P., Hou X., Hou X. D., Chen J. B., *Microchem. J.*, **2018**, *139*, 260
[86] Du H., Yang P., Hou X., Zhou R., Hou X., Chen J., *Chem. Comm.*, **2019**, *55*, 3610
[87] Zhang H., Xu X., Jiang W., *Chem. Sci.*, **2020**, *11*, 7415
[88] Yang K., Wang H., Ma N., Zeng M., Luo H., He D., *ACS Appl. Mater. Interfaces*, **2018**, *10*, 44546
[89] Peng H., Li X. F., Zhang H., Le X. C., *Nat. Commun.*, **2017**, *8*, 14378
[90] Liu C., Hu Y., Pan Q., Yi J., Zhang J., He M., He M., Chen T., Chu X., *Biosens. Bioelectron.*, **2019**, *136*, 31
[91] Liu C., Hu Y., Pan Q., Yi J., Zhang J., He M., He M., Nie C., Chen T., Chu X., *Chem. Comm.*, **2020**, *56*, 3496
[92] Chen K., Huang Q., Fu T., Ke G., Zhao Z., Zhang X., Tan W., *Anal. Chem.*, **2020**, *92*, 7404
[93] Wang J., Wang D. X., Tang A. N., Kong D. M., *Anal. Chem.*, **2019**, *91*, 5244
[94] Yin Y., Chen G., Gong L., Ge K., Pan W., Li N., Machuki J. O., Yu Y., Geng D., Dong H., Gao F., *Anal. Chem.*, **2020**, *92*, 9247
[95] Li H., Gao J., Cao L., Xie X., Fan J., Wang H., Wang H. H., Nie Z., *Angew. Chem. Int. Ed.*, **2021**, *60*, 26001
[96] Chen Y., Wang M., Mao C., *Angew. Chem. Int. Ed.*, **2004**, *43*, 3554
[97] Chen Y., Mao C., *J. Am. Chem. Soc.*, **2004**, *126*, 8626
[98] Chen X. Y., Fu X. R., Wu Y. Y., Jin Y. F., Li W., *Anal. Methods*, **2020**, *12*, 1579
[99] Xiong Z., Wang Q., Zhang J., Yun W., Wang X., Ha X., Yang L., *Spectrochim. Acta A: Mol. Biomol. Spectrosc.*, **2020**, *229*, 118017
[100] He M., He M., Nie C., Yi J., Zhang J., Chen T., Chu X., *ACS Appl. Mater. Interfaces*, **2021**, *13*, 8015
[101] Hu Y., Wang F., Lu C. H., Girsh J., Golub E., Willner I., *Chemistry*, **2014**, *20*, 16203
[102] Li Y. J., Ding X. J., Li D. D., Wu H. P., Huang W., Ding S. J., *Anal. Methods*, **2019**, *11*, 1613
[103] Wen Z. B., Liang W. B., Zhuo Y., Xiong C. Y., Zheng Y. N., Yuan R., Chai Y. Q., *Chem. Comm.*, **2017**, *53*, 7525
[104] Wu Z., Fan H., Satyavolu N. S. R., Wang W., Lake R., Jiang J. H., Lu Y., *Angew. Chem. Int. Ed.*, **2017**, *56*, 8721
[105] Zhang C., Chen J., Sun R., Huang Z., Luo Z., Zhou C., Wu M., Duan Y., Li Y., *ACS Sens.*, **2020**, *5*, 2977
[106] Quan K., Li J., Wang J., Xie N., Wei Q., Tang J., Yang X., Wang K., Huang J., *Chem. Sci.*, **2019**, *10*, 1442
[107] Wei J., Wang H., Wu Q., Gong X., Ma K., Liu X., Wang F., *Angew. Chem. Int. Ed.*, **2020**, *59*, 5965
[108] Wang H., Wang H., Wu Q., Liang M., Liu X., Wang F., *Chem. Sci.*, **2019**, *10*, 9597
[109] Gong K., Wu Q., Wang H., He S., Shang J., Wang F., *Chem. Comm.*, **2020**, *56*, 11410
[110] Zhang D., Ma F., Leng J., Zhang C. Y., *Chem. Comm.*, **2018**, *54*, 13678
[111] Batule B. S., Kim S. U., Mun H., Choi C., Shim W. B., Kim M. G., *J. Agric. Food Chem.*, **2018**, *66*, 3003
[112] Xu J., Qian J., Li H., Wu Z. S., Shen W., Jia L., *Biosens. Bioelectron.*, **2016**, *75*, 41
[113] Park Y., Lee C. Y., Kang S., Kim H., Park K. S., Park H. G., *Nanotechnology*, **2018**, *29*, 085501
[114] Long Y., Zhou C., Wang C., Cai H., Yin C., Yang Q., Xiao D., *Sci. Rep.*, **2016**, *6*, 23949
[115] Xiang B., He K., Zhu R., Liu Z., Zeng S., Huang Y., Nie Z., Yao S., *ACS Appl. Mater. Interfaces*, **2016**, *8*, 22801
[116] Li D., Cheng W., Yan Y., Zhang Y., Yin Y., Ju H., Ding S., *Talanta*, **2016**, *146*, 470
[117] Mi L., Sun Y., Shi L., Li T., *ACS Appl. Mater. Interfaces*, **2020**, *12*, 7879
[118] Ge J., Hu Y., Deng R., Li Z., Zhang K., Shi M., Yang D., Cai R., Tan W., *Anal. Chem.*, **2020**, *92*, 13588
[119] Zhou T., Huang M., Lin J., Huang R., Xing D., *Anal. Chem.*, **2021**, *93*, 2038
[120] Wang X. C., Liu W. W., Yin B. B., Sang Y. W., Liu Z. P., Dai Y., Duan X. Z., Zhang G., Ding S. J., Tao Z. H., *Microchim Acta*, **2017**, *184*, 1603
[121] Zhou D. H., Wu W., Li Q., Pan J. F., Chen J. H., *Anal. Methods*, **2019**, *11*, 3546
[122] Orbach R., Remacle F., Levine R. D., Willner I., *Proc. Natl. Acad. Sci. USA*, **2012**, *109*, 21228
[123] Lilienthal S., Klein M., Orbach R., Willner I., Remacle F., Levine R. D., *Chem. Sci.*, **2017**, *8*, 2161
[124] Zhang J., Lu Y., *Angew. Chem. Int. Ed.*, **2018**, *57*, 9702
[125] Chen F., Bai M., Cao K., Zhao Y., Cao X., Wei J., Wu N., Li J., Wang L., Fan C., Zhao Y., *ACS Nano*, **2017**, *11*, 11908
[126] Qian R. C., Zhou Z. R., Guo W., Wu Y., Yang Z., Lu Y., *J. Am. Chem. Soc.*, **2021**, *143*, 5737
[127] Shlyahovsky B., Li Y., Lioubashevski O., Elbaz J., Willner I., *ACS Nano*, **2009**, *3*, 1831
[128] Zhu J., Zhang L., Li T., Dong S., Wang E., *Adv. Mater.*, **2013**, *25*, 2440
[129] Chen J., Pan J., Chen S., *Chem. Sci.*, **2018**, *9*, 300
[130] Chen J., Pan J., Liu C., *Anal. Chem.*, **2020**, *92*, 6173
[131] Haydell M. W., Centola M., Adam V., Valero J., Famulok M., *J. Am. Chem. Soc.*, **2018**, *140*, 16868
[132] Bi S., Yan Y., Hao S., Zhang S., *Angew. Chem. Int. Ed.*, **2010**, *49*, 4438
[133] Zhang C., Yang J., Jiang S., Liu Y., Yan H., *Nano Lett.*, **2016**, *16*, 736
[134] Wang J., Zhou Z., Li Z., Willner I., *Chem. Sci.*, **2020**, *12*, 341

[135] Wang J., Li Z., Willner I., *Nat. Commun.*, **2022**, *13*, 4414
[136] Dong J., Ouyang Y., Wang J., O'Hagan M. P., Willner I., *ACS Nano*, **2022**, *16*, 6153
[137] Li Z., Wang J., Zhou Z., O'Hagan M. P., Willner I., *ACS Nano*, **2022**, *16*, 3625
[138] Wang S., Yue L., Shpilt Z., Cecconello A., Kahn J. S., Lehn J. M., Willner I., *J. Am. Chem. Soc.*, **2017**, *139*, 9662
[139] Zhou Z., Yue L., Wang S., Lehn J. M., Willner I., *J. Am. Chem. Soc.*, **2018**, *140*, 12077
[140] Yue L., Wang S., Willner I., *J. Am. Chem. Soc.*, **2019**, *141*, 16461
[141] Yue L., Wang S., Lilienthal S., Wulf V., Remacle F., Levine R. D., Willner I., *J. Am. Chem. Soc.*, **2018**, *140*, 8721
[142] Wang S., Yue L., Li Z. Y., Zhang J., Tian H., Willner I., *Angew. Chem. Int. Ed.*, **2018**, *57*, 8105
[143] Wang Z., Yang J., Qin G., Zhao C., Ren J., Qu X., *Angew. Chem. Int. Ed.*, **2022**, *61*, e202204291
[144] Jerome C. A., Hoshika S., Bradley K. M., Benner S. A., Biondi E., *Proc. Natl. Acad. Sci. USA*, **2022**, *119*, e2208261119
[145] Chen L., Luo S., Ge Z., Fan C., Yang Y., Li Q., Zhang Y., *Nano Lett.*, **2022**, *22*, 1618
[146] Zhao X., Wang Y., Jiang W., Wang Q., Li J., Wen Z., Li A., Zhang K., Zhang Z., Shi J., Liu J., *Adv. Mater.*, **2022**, *34*,
[147] Li Y., Chang Y., Ma J., Wu Z., Yuan R., Chai Y., *Anal. Chem.*, **2019**, *91*, 6127
[148] Huang Y., Lin C., Luo F., Qiu B., Guo L., Lin Z., Chen G., *ACS Sens.*, **2019**, *4*, 2465
[149] Si H., Sheng R., Li Q., Feng J., Li L., Tang B., *Anal. Chem.*, **2018**, *90*, 8785
[150] Yang Z., Loh K. Y., Chu Y. T., Feng R., Satyavolu N. S. R., Xiong M., Nakamata Huynh S. M., Hwang K., Li L., Xing H., Zhang X., Chemla Y. R., Gruebele M., Lu Y., *J. Am. Chem. Soc.*, **2018**, *140*, 17656
[151] Yang C., Yin X., Huan S. Y., Chen L., Hu X. X., Xiong M. Y., Chen K., Zhang X. B., *Anal. Chem.*, **2018**, *90*, 3118
[152] Cui M. R., Li X. L., Xu J. J., Chen H. Y., *ACS Appl. Mater. Interfaces*, **2020**, *12*, 13005
[153] Lin Y., Yang Z., Lake R. J., Zheng C., Lu Y., *Angew. Chem. Int. Ed.*, **2019**, *58*, 17061
[154] Xiong M., Yang Z., Lake R. J., Li J., Hong S., Fan H., Zhang X. B., Lu Y., *Angew. Chem. Int. Ed.*, **2020**, *59*, 1891
[155] Wu Y., Meng H. M., Chen J., Jiang K., Yang R., Li Y., Zhang K., Qu L., Zhang X. B., Li Z., *Chem. Comm.*, **2020**, *56*, 470
[156] Xu Y., Lu Z., Fu X., Yu F., Chen H., Nie Y., *Sensors & Actuators B: Chemical*, **2020**, *306*, 127549
[157] Li C., Xue C., Wang J., Luo M., Shen Z., Wu Z. S., *Anal. Chem.*, **2019**, *91*, 11529
[158] Zhang J., He M., Nie C., He M., Pan Q., Liu C., Hu Y., Yi J., Chen T., Chu X., *Anal. Chem.*, **2019**, *91*, 9049
[159] Zhu D., Wei Y., Sun T., Zhang C., Ang L., Su S., Mao X., Li Q., Fan C., Zuo X., Chao J., Wang L., *Anal. Chem.*, **2021**, *93*, 2226
[160] Meng X., Zhang K., Yang F., Dai W., Lu H., Dong H., Zhang X., *Anal. Chem.*, **2020**, *92*, 8333
[161] Zhang T. T., Peng Y., Yuan R., Xiang Y., *Sensors & Actuators B: Chemcial*, **2018**, *273*, 70
[162] Yang Y., Huang J., Yang X., Quan K., Wang H., Ying L., Xie N., Ou M., Wang K., *Anal. Chem.*, **2016**, *88*, 5981
[163] Fu X., Ke G., Peng F., Hu X., Li J., Shi Y., Kong G., Zhang X. B., Tan W., *Nat. Commun.*, **2020**, *11*, 1518
[164] Xu Y. T., Ruan Y. F., Wang H. Y., Yu S. Y., Yu X. D., Zhao W. W., Chen H. Y., Xu J. J., *Small*, **2021**, *17*, e2100503
[165] Li J., Wang S., Jiang B., Xiang Y., Yuan R., *Analyst*, **2019**, *144*, 2430
[166] Li C., Ma J., Shi H., Hu X., Xiang Y., Li Y., Li G., *Anal. Chim. Acta*, **2018**, *1041*, 102
[167] Liu C., Zhang S., Li X., Xue Q., Jiang W., *Analyst*, **2019**, *144*, 4241
[168] Gao T., Chai W., Shi L., Shi H., Sheng A., Yang J., Li G., *Analyst*, **2019**, *144*, 6365
[169] Zhang R., Wang Y., Qu X., Li S., Zhao Y., Zhang F., Liu S., Huang J., Yu J., *Analyst*, **2019**, *144*, 4995
[170] Wang Y., Yang L., Wang Y., Liu W., Li B., Jin Y., *Analyst*, **2019**, *144*, 5959
[171] Feng C., Wang Z., Chen T., Chen X., Mao D., Zhao J., Li G., *Anal. Chem.*, **2018**, *90*, 2810
[172] Wang W. J., Shu M. B., Nie A. X., Han H. Y., *Sensors & Actuators B: Chemical*, **2020**, *304*, 127380
[173] Shiu S. C., Cheung Y. W., Dirkzwager R. M., Liang S., Kinghorn A. B., Fraser L. A., Tang M. S. L., Tanner J. A., *Adv. Biosyst.*, **2017**, *1*, e1600006
[174] Shang J., Li C., Li F., Wang Q., Yuan B., Wang F., *Anal. Chem.*, **2021**, *93*, 2403
[175] Zhou W., Ding J., Liu J., *Theranostics*, **2017**, *7*, 1010
[176] Taylor A. I., Wan C. J. K., Donde M. J., Peak-Chew S.-Y., Holliger P., *Nat. Chem.*, **2022**, *14*, 1295
[177] Qian R.-C., Zhou Z.-R., Wu Y., Yang Z., Guo W., Li D.-W., Lu Y., *Angew. Chem. Int. Ed.*, **2022**, *61*, e202210935
[178] Singh N., Ranjan A., Sur S., Chandra R., Tandon V., *J. Biosci. Bioeng.*, **2012**, *37*, 493
[179] Yu L., Chen Y., Lin H., Gao S., Chen H., Shi J., *Small*, **2018**, *14*, e1800708
[180] Bhindi R., Fahmy R. G., Lowe H. C., Chesterman C. N., Dass C. R., Cairns M. J., Saravolac E. G., Sun L. Q., Khachigian L. M., *Am. J. Pathol.*, **2007**, *171*, 1079
[181] Kole R., Krainer A. R., Altman S., *Nat. Rev. Drug Discov.*, **2012**, *11*, 125
[182] Nedorezova D. D., Fakhardo A. F., Nemirich D. V., Bryushkova E. A., Kolpashchikov D. M., *Angew. Chem. Int. Ed.*, **2019**, *58*, 4654
[183] Thai H. B. D., Levi-Acobas F., Yum S. Y., Jang G., Hollenstein M., Ahn D. R., *Chem. Comm.*, **2018**, *54*, 9410
[184] Meng L., Ma W., Lin S., Shi S., Li Y., Lin Y., *ACS Appl. Mater. Interfaces*, **2019**, *11*, 6850
[185] Fan H., Zhao Z., Yan G., Zhang X., Yang C., Meng H., Chen Z., Liu H., Tan W., *Angew. Chem. Int. Ed.*, **2015**, *54*, 4801
[186] Yi J. T., Pan Q. S., Liu C., Hu Y. L., Chen T. T., Chu X., *Nanoscale*, **2020**, *12*, 10380
[187] Liu S. Y., Xu Y., Yang H., Liu L., Zhao M., Yin W., Xu Y. T., Huang Y., Tan C., Dai Z., Zhang H., Zhang J. P., Chen X. M., *Adv. Mater.*, **2021**, *33*, e2100849
[188] Jin Y., Wang H., Li X., Zhu H., Sun D., Sun X., Liu H., Zhang Z., Cao L., Gao C., Wang H., Liang X. J., Zhang J., Yang X., *ACS Appl. Mater. Interfaces*, **2020**, *12*, 26832
[189] Henderson B. W., Dougherty T. J., *Photochem. Photobiol.*, **1992**, *55*, 145
[190] Moan J., Berg K., *Photochem. Photobiol.*, **1992**, *55*, 931
[191] Li W., Ma Q. Y., Wu E. X., *Int. J. Photoenergy*, **2012**, *2012*, 1
[192] Agostinis P., Berg K., Cengel K. A., Foster T. H., Girotti A. W., Gollnick S. O., Hahn S. M., Hamblin M. R., Juzeniene A., Kessel D., Korbelik M., Moan J., Mroz P., Nowis D., Piette J., Wilson B. C., Golab J., *CA Cancer J. Clin.*, **2011**, *61*, 250
[193] Robinson J. T., Tabakman S. M., Liang Y., Wang H., Casalongue H. S., Vinh D., Dai H., *J. Am. Chem. Soc.*, **2011**, *133*, 6825
[194] Cheng L., Gong H., Zhu W., Liu J., Wang X., Liu G., Liu Z., *Biomaterials*, **2014**, *35*, 9844
[195] Feng J., Xu Z., Liu F., Zhao Y., Yu W., Pan M., Wang F., Liu X., *ACS Nano*, **2018**, *12*, 12888
[196] Lin H., Chen Y., Shi J., *Chem. Soc. Rev.*, **2018**, *47*, 1938
[197] Lin L. S., Song J., Song L., Ke K., Liu Y., Zhou Z., Shen Z., Li J., Yang Z., Tang W., Niu G., Yang H. H., Chen X., *Angew. Chem. Int. Ed.*, **2018**, *57*, 4902
[198] Sang Y., Cao F., Li W., Zhang L., You Y., Deng Q., Dong K., Ren J., Qu X., *J. Am. Chem. Soc.*, **2020**, *142*, 5177
[199] Li Y., Zhao P., Gong T., Wang H., Jiang X., Cheng H., Liu Y., Wu Y., Bu W., *Angew. Chem. Int. Ed.*, **2020**, *59*, 22537
[200] Liu C., Chen Y., Zhao J., Wang Y., Shao Y., Gu Z., Li L., Zhao Y., *Angew. Chem. Int. Ed.*, **2021**, *60*, 14324
[201] Li X., Hu H., Shi Y., Liu Y., Zhou M., Huang Z., Li J., Ke G., Chen M., Zhang X.-B., *Chem. Eur. J.*, **2023**, https://doi.org/10.1002/chem.202203227
[202] Zhou M., Yin Y., Shi Y., Huang Z., Shi Y., Chen M., Ke G., Zhang X.-B., *Chem. Comm.*, **2022**, *58*, 4508
[203] Tu T., Huan S., Ke G., Zhang X., *Chem. Res. Chinece Universities*, **2022**, *38*(4), 912
[204] Kong G., Xiong M., Liu L., Hu L., Meng H.-M., Ke G., Zhang X.-B., Tan W., *Chem. Soc. Rev.*, **2021**, *50*, 1846
[205] Fu X., Shi Y., Peng F., Zhou M., Yin Y., Tan Y., Chen M., Yin X., Ke G., Zhang X.-B., *Anal. Chem.*, **2021**, *93*, 4967